Stratigraphic and microfossil evidence for a 4500-year history of Cascadia subduction zone earthquakes and tsunamis at Yaquina River estuary, Oregon, USA

Nicholas A. Graehl[1], Harvey M. Kelsey[2,†], Robert C. Witter[3], Eileen Hemphill-Haley[2], and Simon E. Engelhart[4]
[1]*Lettis Consultants International, Inc., 4155 Darley Avenue, Suite A, Boulder, Colorado 80305, USA*
[2]*Department of Geology, Humboldt State University, Arcata, California 95524, USA*
[3]*U.S. Geological Survey, Alaska Science Center, 4210 University Drive, Anchorage, Alaska 99508, USA*
[4]*Department of Geosciences, University of Rhode Island, 9 E. Alumni Avenue, Kingston, Rhode Island 02881, USA*

ABSTRACT

The Sallys Bend swamp and marsh area on the central Oregon coast onshore of the Cascadia subduction zone contains a sequence of buried coastal wetland soils that extends back ~4500 yr B.P. The upper 10 of the 12 soils are represented in multiple cores. Each soil is abruptly overlain by a sandy deposit and then, in most cases, by greater than 10 cm of mud. For eight of the 10 buried soils, times of soil burial are constrained through radiocarbon ages on fine, delicate detritus from the top of the buried soil; for two of the buried soils, diatom and foraminifera data constrain paleoenvironment at the time of soil burial.

We infer that each buried soil represents a Cascadia subduction zone earthquake because the soils are laterally extensive and abruptly overlain by sandy deposits and mud. Preservation of coseismically buried soils occurred from 4500 yr ago until ~500–600 yr ago, after which preservation was compromised by cessation of gradual relative sea-level rise, which in turn precluded drowning of marsh soils during instances of coseismic subsidence. Based on grain-size and microfossil data, sandy deposits overlying buried soils accumulated immediately after a subduction zone earthquake, during tsunami incursion into Sallys Bend. The possibility that the sandy deposits were sourced directly from landslides triggered upstream in the Yaquina River basin by seismic shaking was discounted based on sedimentologic, microfossil, and depositional site characteristics of the sandy deposits, which were inconsistent with a fluvial origin. Biostratigraphic analyses of sediment above two buried soils—in the case of two earthquakes, one occurring shortly after 1541–1708 cal. yr B.P. and the other occurring shortly after 3227–3444 cal. yr B.P.—provide estimates that coseismic subsidence was a minimum of 0.4 m. The average recurrence interval of subduction zone earthquakes is 420–580 yr, based on an ~3750–4050-yr-long record and seven to nine interearthquake intervals.

The comparison of the Yaquina Bay earthquake record to similar records at other Cascadia coastal sites helps to define potential patterns of rupture for different earthquakes, although inherent uncertainty in dating precludes definitive statements about rupture length during earthquakes. We infer that in the first half of the last millennia, the northern Oregon part of the subduction zone had a different rupture history than the southern Oregon part of the subduction zone, and we also infer that at ca. 1.6 ka, two earthquakes closely spaced in time together ruptured a length of the megathrust that extends at least from southwestern Washington to southern Oregon.

INTRODUCTION

Approximately 25 yr ago, Atwater (1987) first published convincing evidence that the Cascadia subduction zone (Fig. 1) ruptured in great earthquakes. While much remains to be determined about earthquake sizes and recurrence intervals, an emerging consensus based on decades of research that addresses the paleoseismic history of the Cascadia subduction zone is that subduction zone earthquakes occur with regularity, and recurrence intervals, based on sites with >2500 yr of record, range from a few centuries to a millennium (Atwater and Hemphill-Haley, 1997; Kelsey et al., 2002; Witter et al., 2003; Nelson et al., 2006). Some subduction zone earthquakes in all likelihood ruptured the entire margin, but others did not (Nelson et al., 2006; Goldfinger et al., 2012). Tsunami waves accompanied these subduction zone earthquakes and left depositional evidence in both coseismically subsided wetlands and coastal lakes (Witter et al., 2003; Kelsey et al., 2005). However, as is the case with efforts to better characterize tectonics of a particular subduction zone, ongoing research can both clarify uncertainties and invite clarification of new emerging uncertainties.

From a 25 yr perspective, the following emerging data requirements and unresolved questions provided a framework for our paleoseismic research on the Yaquina River estuary in central coastal Oregon. First, there is a need for longer historical records of subduction zone earthquakes along the central and northern Oregon coast. Existing studies on the central and northern Oregon coast provide earthquake history going back less than 2000 yr (Darienzo et al., 1994; Shennan et al., 1998; Nelson et al., 1995, 2004; Witter, 2008; Witter et al., 2009), whereas studies on the southern Washington coast and the Columbia River embayment to the north and the southern Oregon coast to the south (Fig. 1) have produced earthquake records going back 5000 and more than 6000 yr, respectively (Shennan et al., 1996; Atwater and Hemphill-Haley, 1997; Kelsey et al., 2002; Witter et al., 2003; Atwater et al., 2004). Second, the use of paleogeodetic techniques tied to diatom and foraminiferal biostratigraphy (e.g., Hawkes et al., 2011; Engelhart et al., 2013a) can provide better constraints on the amount of coseismic subsidence for more paleoearthquakes. The amount of coseismic subsidence is an important constraint on rupture models (e. g., Leonard et al., 2010; Wang et al., 2013). Third, although it is clear that tsunamis accompany

[†]E-mail: hmk1@humboldt.edu.

GSA Bulletin; January/February 2015; v. 127; no. 1/2; p. 211–226; doi: 10.1130/B31074.1; 12 figures; 3 tables; Data Repository item 2014282; published online 7 August 2014.

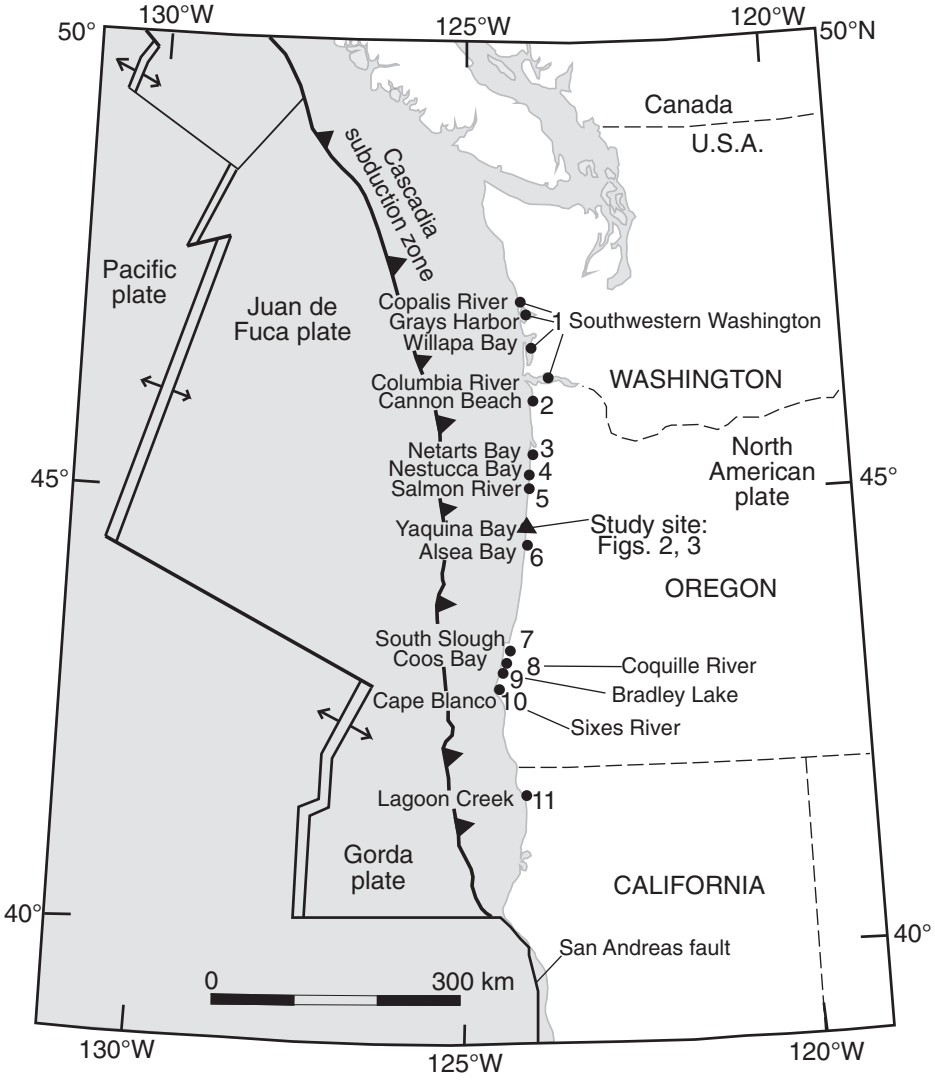

Figure 1. Location of Yaquina Bay (black triangle, see detailed map in Fig. 2) on the central Oregon coast within the context of the Cascadia subduction zone. The Juan de Fuca plate is obliquely subducting northeast beneath the North American plate at ~40 mm/yr. The Cascadia deformation front (barbed line), located at the bathymetric boundary between the western edge of the continental slope and the abyssal plain, is ~90 km offshore from Yaquina Bay. Black dots along coastline locate paleoseismic investigation sites that are mentioned in text. 1—southwestern Washington and Columbia River embayment (Atwater et al., 2004); 2—Cannon Beach (Witter, 2008), 3—Netarts Bay (Darienzo et al., 1994; Nelson et al., 1995; Shennan et al., 1998), 4—Nestucca Bay (Witter et al., 2009), 5—Salmon River (Nelson et al., 1995, 2004); 6—Alsea Bay (Nelson et al., 2008); 7—South Slough within Coos Bay (Nelson et al., 1996a, 1998); 8—Coquille River (Witter et al., 2003); 9—Bradley Lake (Kelsey et al., 2005); 10—Sixes River (Kelsey et al., 2002); and 11—Lagoon Creek (Abramson, 1998; Garrison-Laney, 1998).

major Cascadia subduction zone earthquakes, what is less clear is how tsunami deposits can be clearly distinguished from similar-textured tidal flat or flood deposits in the years to decades after a subduction zone earthquake. Such distinctions are critical in order to appropriately employ biostratigraphic data in paleogeodetic determinations. Fourth, and finally, there is the ongoing need to collect paleoseismic data that, when cumulatively added to a growing archive of such data, potentially can better address the question of when, where, and how often the Cascadia subduction zone breaks in shorter ruptures that do not involve coseismic displacement of the whole length of the megathrust. Our results make progress in addressing all four issues.

In paleoseismic research in coastal Oregon that was a precursor to subsequent, more detailed work at Yaquina Bay, Darienzo (1991) made the case that buried soils in northern Oregon estuaries were an archive of past subduction zone earthquakes, and he used criteria of widespread episodes of submergence, abrupt upper contacts of buried marsh surfaces, and fossil diatom assemblages consistent with abrupt submergence as evidence for an earthquake origin to soil burial. The subsequent paleoseismic investigations by Darienzo et al. (1994), Darienzo and Peterson (1995), and Peterson and Priest (1995) in Yaquina River estuary established that as many as seven buried soils are present along the lower 25.5 km of the river, with at least three of these buried soils having sand deposits directly overlying them (Fig. 2A). Because the head of tide extends 26 km up the Yaquina River, these paleoseismic investigations extended the full length of the estuarine tidal reach. From these buried soil observations, Darienzo and Peterson (1995) estimated that the average recurrence interval between times of coseismic subsidence of soils, spanning five intervals, was 360–590 yr.

In a reconnaissance survey of paleotsunami deposits in Yaquina Bay, Peterson and Priest (1995) inferred that as many as 14 marsh sites in the lower 15 km of the Yaquina Bay estuary showed evidence of tsunamis, manifest as sand layers immediately above buried soils. The inferred tsunami deposits represented at least three plate-boundary earthquakes.

At the onset of this investigation, reconnaissance field investigations at eight marsh locations along the lower 24 km of Yaquina River (Fig. 2B; Data Repository[1]) were carried out, using previous work as a partial guide, in order to determine the best possible location for an in-depth site investigation. Ultimately, field investigations were focused at a freshwater marsh and spruce swamp that fringes the northeast shore of the Sallys Bend embayment in the lower Yaquina River estuary. Peterson and Priest (1995) previously examined a core at this site, which they named Sallys Bend; we adopt Sallys Bend as the study site name (Fig. 2B).

In this paper, we address the following objectives. First, we describe a >4000 yr record of subduction zone earthquakes deduced from coastal stratigraphy at Sallys Bend, Yaquina Bay. Second, we determine buried-soil–specific

[1]GSA Data Repository item 2014282, Tables DR1 and DR2, and Figures DR1 through DR7, which summarize location and stratigraphic data for reconnaissance cores in Yaquina Bay and locations for the focus cores at Sallys Bend, is available online at www.geosociety.org/pubs/ft2014.htm, or on request from editing@geosociety.org or Documents Secretary, GSA, P.O. Box 9140, Boulder, CO 80301, USA.

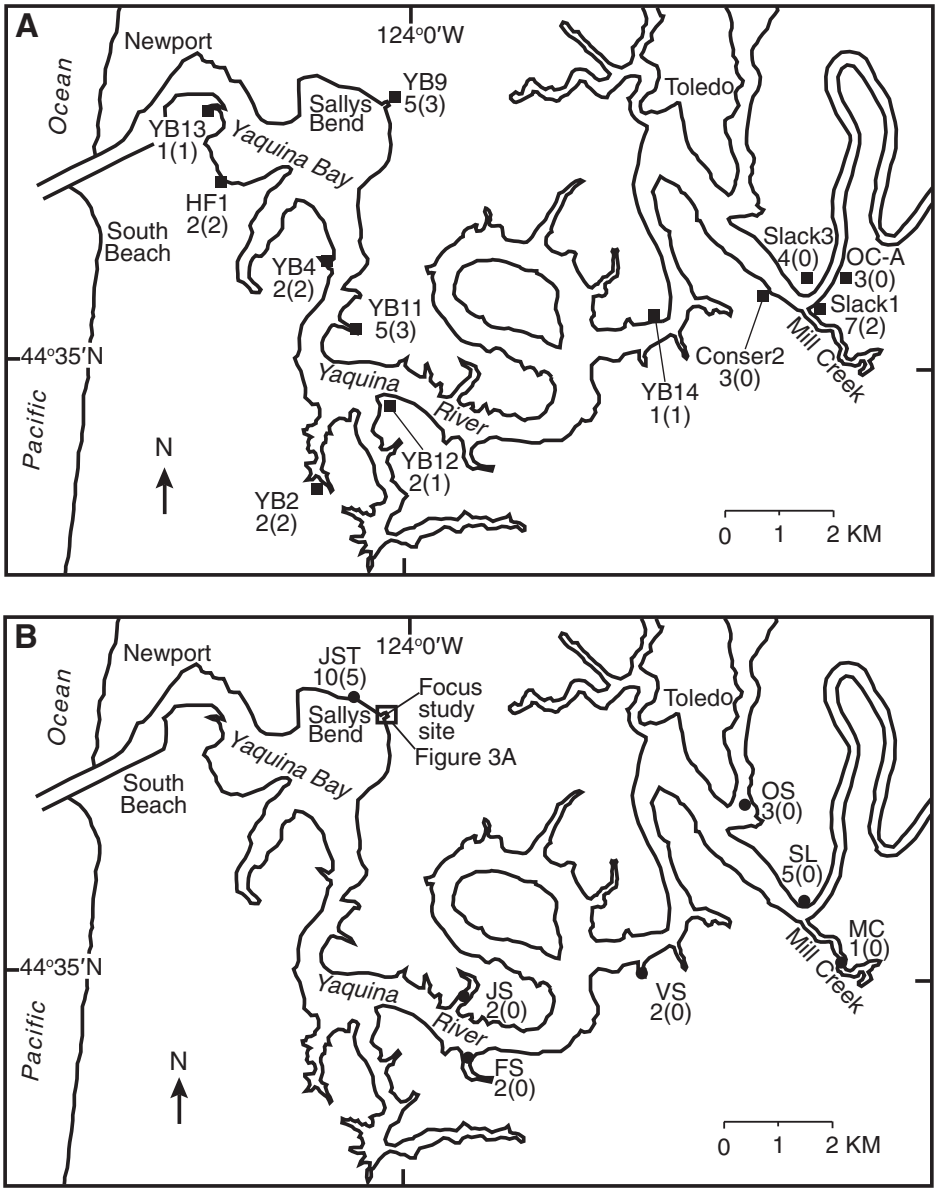

Figure 2. (A) Yaquina Bay, Oregon, showing selected core site locations from previous work of Darienzo et al. (1994), Darienzo and Peterson (1995), and Peterson and Priest (1995). For these sites, the first number after the core site identification number is the number of buried soils observed, followed in parentheses by a number indicating the number of sand layers observed above buried soils. (B) Map of Yaquina Bay and lower Yaquina River showing the location of the Sallys Bend research site. Black dots are locations of reconnaissance sites for this study: JST—Johnston Slough; JS—Johnson Slough; VS—Van Eck Slough; FS—Flesher Slough; OS—Olalla Slough; MC—Mill Creek; and SL—Slack Slough. The first number after the core site identification number is the number of buried soils observed, followed in parentheses by a number indicating the number of sand layers observed above buried soils. For the reconnaissance core sites, coordinate site locations (Tables DR1–DR2) and core stratigraphy (Figs. DR1–DR7) are contained in the Date Repository (see text footnote 1).

estimates of the amount of coseismic subsidence during two earthquakes. Third, we provide biostratigraphic and grain-size data for sandy deposits overlying buried soils, which in turn enable more informed understanding of the origin of such deposits. Finally, through employing the additional earthquake site chronology at Yaquina Bay, we address the question of length of ruptures for earthquakes along the Cascadia subduction zone.

RESEARCH APPROACH

Three approaches were used to determine whether or not buried soils and overlying sandy deposits at Sallys Bend record late Holocene Cascadia earthquakes. The first approach involved describing subsurface stratigraphy at multiple core sites, the second entailed radiometric dating of strata proximal to mud-over-peat contacts to assess the time of soil burial, and the third involved analyzing diatom and foraminiferal assemblages to assess paleoenvironmental changes that accompanied burial of soils.

The stratigraphy of Sallys Bend swamp and marsh was investigated at 10 core sites (Fig. 3A) using 2.5-cm-diameter gouge cores. Larger-diameter (6 cm) core samples were taken for radiometric and biostratigraphic analyses. All core samples were photographed and then described in the field using the Troels-Smith classification for organic and mineral deposits (Troels-Smith, 1955). Subsequent unit descriptions, employed in this paper, are derivatives of the Troels-Smith field descriptions. Stratigraphic units include peat, muddy peat, peaty mud, or mud, depending on field estimates of relative amounts of organic and mineral fractions. The percent organics by volume for peat, muddy peat, and peaty mud are 100%–75%, 75%–50%, and 50%–25%, respectively. "Mud" refers to clayey silts in which organics total <25% by volume. Finally, a stratigraphic unit common to most all cores was a relatively coarse inorganic unit consisting of very fine sandy silt or silty very fine sand.

Core locations and elevations at Sallys Bend were determined using a total station with survey loops (survey closure ≤10 mm) tied to a temporary benchmark on the adjacent Yaquina Bay Road. The vertical position of the temporary benchmark (NAVD88 datum) was then tied to National Oceanic and Atmospheric Administration (NOAA) tidal station 9435380 in South Beach, Oregon (Fig. 2A; NOAA-COOPS, 2012) using a real-time kinematic differential global positioning system with a vertical accuracy of ±20 mm. Therefore, all core sites are referenced relative to the mean lower low water (MLLW) tidal datum.

Radiocarbon samples were collected with the intent of determining the age of soil burial. Samples came from detrital organic fragments within the uppermost 1 to 2 cm of a buried soil or directly above the buried soil. Sample material avoided charcoal fragments, and only four detrital sample types were considered suitable for analysis: seeds, spruce needles, spruce cones, and <1.5-mm-diameter twigs with protruding nodes that would be broken up by significant

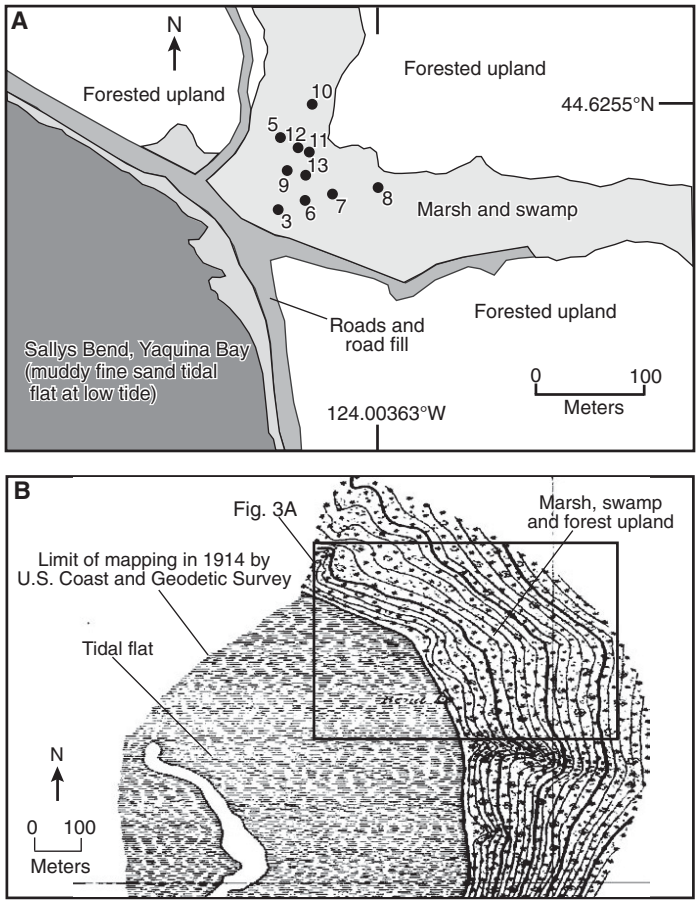

Figure 3. (A) Map of Sallys Bend showing the 10 core site locations. (B) U.S. Coast and Geodetic Survey T-sheet number T03489 showing the shoreline character of Sallys Bend as mapped by J.W. Maupin in 1914 prior to bay margin road construction and diking. Similar to the present time, the Sallys Bend core site was a swamp and marsh at the edge of the forest upland and not in the tidal zone. Source: specialprojects.nos.noaa.gov/tools/shorelinesurvey.html.

transport. Transport would break up needles, cones, and delicate twigs; seeds, although less susceptible to being broken down by transport, are disseminated by transport and become too sparse to be successfully sampled.

Radiocarbon sample material was extracted from a 1 mm sieve, picked clean of modern roots and sediment, washed with distilled water, air dried, and submitted for analysis. Radiocarbon AMS (accelerator mass spectrometry) ages were determined by Beta Analytic, Inc. Laboratory-reported ages were then calibrated using CALIB version 7.0 (Stuiver and Reimer, 1993) and the IntCal13 data set (Reimer et al., 2013). All calibrated ages are reported as age ranges at two standard deviations in "cal. yr B.P." (B.P., before present), where "present" is A.D. 1950.

In one core, diatom assemblages were used to assess paleoenvironmental changes across the sharp upper contacts of two buried soils. Diatom samples were processed to remove clays and organic material. The diatom samples were mounted to glass slides, and diatoms were identified to species level whenever possible. Abundance data (counts greater than 100 valves per sample in addition to the prolific and resilient genus *Paralia*) were tabulated to quantitatively compare diatom presence and amount among samples.

In the absence of local modern surface transect data to develop transfer functions for diatoms (e.g., Sawai et al., 2004; Nelson et al., 2008), we incorporated information from existing studies for modern intertidal diatoms at Pacific Northwest coastal sites. These sites include Yaquina Bay (including the tidal flat at Sallys Bend; Riznyk, 1973), Alsea Bay (Nelson et al., 2008), and other localities in the Pacific Northwest (Hemphill-Haley, 1995; Atwater and Hemphill-Haley, 1997). Species taxonomy and inferred environments for diatom assemblages are additionally based on data sets in Hemphill-Haley (1995) and Atwater and Hemphill-Haley (1997). Paleoenvironments are assigned to tidal flat, low marsh, high marsh, or an upland/freshwater zone. The upland or freshwater environment is characterized by a lack of diatoms or by presence of diatoms that are inconsistent with brackish intertidal depositional environments. Diatom preservation was documented as an aid to the interpretation of the conditions of deposition.

Similarly, for the foraminiferal analyses, a replicate core was recovered adjacent to the core used for the diatom analyses. The core was cut into 1-cm-thick slices along a 20-cm-depth interval that had been sampled in an adjacent core for diatoms. The sediment was then wet-sieved to retain the 500–63 μm size fraction. Samples were inspected under a binocular microscope until 100 individuals had been counted or the entire sample was analyzed. Species taxonomy is based on Hawkes et al. (2011) and Engelhart et al. (2013a). Inferred environments for the foraminiferal assemblages are based on the combined data set of Engelhart et al. (2013b).

RESULTS

Core Stratigraphy and Buried Soils

As observed in cores, buried soils are dark organic-rich horizons that are peat or peaty mud. Organic material in the buried soils contained traces of forest litter, including spruce needles, tree cones, and small twigs. Younger buried soils typically were more fibrous and less humified than older soils.

Ten cores in Sallys Bend together document the occurrence of 12 buried soils (Table 1), and the buried soils are correlated among cores based on depth in core and thickness of the overlying mud unit (Figs. 4 and 5; Table 1). The two oldest and deepest-buried soils (L and K; Figs. 4 and 5) are represented in relatively few cores. Soil L is only observed in cores 8 and 9, and soil K is only observed in cores 3, 8, 9, 11, and 12 (Figs. 4 and 5). Two of the shallowest-buried soils, buried soils B and D, are thin and have minimal (<10 cm thick) overlying mud units (Figs. 4 and 5; Table 1). However, the remaining eight buried soils (that is, A, C, E, F, G, H, I, J) are well expressed in at least 7 of the 10 cores and have overlying mud units more than 10 cm thick (Figs. 4 and 5), indicating long-lasting submergence after the burial of the soil. All the buried soils, whether well represented among multiple cores or not, had dominantly sharp (<1 mm to 3 mm) contacts between the buried soils and the overlying unit (Table 1).

TABLE 1. BURIED SOIL ATTRIBUTES

Buried soil (number of cores that sample the buried soil)	Depth range (mean depth) to top of buried soil (cm)	Nature of upper contact of buried soil*	Number of cores that contain sandy deposit overlying buried soil	Thickness range (mean thickness) of sandy deposit overlying buried soil (cm)	Number of cores that have mud deposit overlying buried soil	Thickness range (mean thickness) of mud deposit overlying buried soil (cm)
A (9)	23–63 (51)	8s, 3c, 1g	5	5–24 (11)	8	7–29 (18)
B (8)	52–100 (77)	5s, 4c	4	0.2–30 (9)	6	2–9 (6)
C (10)	122–174 (151)	13s, 1c	10	1–68 (19)	6	11–47 (24)
D (5)	166–221 (191)	5s	0	No	5	1–4 (3)
E (9)	176–264 (232)	9s, 2c	3	3–5 (4)	8	0.5–32 (11)
F (10)	254–307 (291)	10s, 3c	6	0.5–9 (4)	10	1–62 (20)
G (7)	303–376 (349)	10s	7	2–13 (4)	7	4–20 (11)
H (9)	391–459 (421)	13s, 1c	6	1–35 (13)	9	13–44 (30)
I (7)	404–504 (467)	11s	7	1–4 (3)	5	3–48 (26)
J (7)	524–583 (545)	8s	4	5–8 (6)	7	24–177 (64)
K (4)	560–638 (588)	5s	2	2 (2)	2	4–7 (5)
L (2)	620–665 (653)	2s	0	No	2	15–48 (32)

Note: Depths and thicknesses are rounded to nearest centimeter; thicknesses <1 cm are rounded to nearest millimeter. No—not observed.
*Contacts: s—sharp, <3 mm; c—clear, >3–10 mm; g—gradual, >10 mm. Numbers refer to number of observations.

Mud, or a slightly coarser sandy deposit, overlies the buried soils. The texture of the relatively coarse deposit that often overlies the buried soils ranges from silty fine sand to fine sandy silt, but for ease of subsequent discussion, we will refer to these deposits as "sandy deposits overlying buried soils." Although there is not an abundance of sandy deposits in the cores, when sandy deposits do occur, they directly overlie buried soils (Figs. 4 and 5). A few of the buried soils (soils B and D) have minimal sandy deposits overlying the buried soil, but other buried soils (soils C, G, H, and I) have sandy deposits overlying the buried soil in most cores. An additional stratigraphic unit, which is uncommon but notable (only two instances observed), is ~30-cm-thick mud intervals that contain 0.5- to 5.0-mm-thick laminations of either very fine sand or organics (Fig. 5).

The core sites are either proximal, intermediate, or distal relative to the edge of the modern tidal flat to the southwest (Figs. 4 and 5), and the thickness of sandy deposits overlying buried soils reflects core proximity to the tidal flat. The one core most proximal to the edge of the tidal flat (core 3) has thick sandy deposits (up to 30 cm) above buried soils (Figs. 4 and 5). At the other extreme, the two cores most distal to the edge of the tidal flat (cores 8 and 10) have no sandy deposits (core 10) or minimal sandy deposits overlying buried soils (core 8) (Figs. 4 and 5). The cores that are intermediate in distance inland from the edge of the tidal flat have variable thicknesses of sandy deposits above the buried soils, and these variable thicknesses are intermediary between the relatively thick sandy deposits that overlie soils in core 3 and the thinner to nonexistent sandy deposits that overlie soils in cores 8 and 10 (Figs. 4 and 5). Although the thickness of the sandy deposits overlying buried soils generally decreases inland, the most graphic example is soil H, where the overlying sandy deposit systematically thins inland from the tidal flat (Fig. 5).

Sandy Deposit Overlying Buried Soils: Diatom, Foraminiferal, and Grain-Size Analysis

At the core 11 site (Fig. 3), we sampled buried soil C and the overlying sandy deposit for grain size, foraminifera, and diatoms (Figs. 6, 7, and 8); in addition, we sampled buried soil G and the overlying sandy deposit for diatoms (Fig. 9). Soils C and G were chosen because both buried soils have organic detritus diagnostic of an upland forest environment, are overlain by a sandy deposit, and are overlain in turn by a mud interval that in all cores is at least 10 cm thick.

For buried soil C, there was an erosive, sharp contact between soil C and the overlying sandy sediment, which consists of ~8 cm of silty fine to very fine sand to fine to very fine sandy silt that transitions upward to mud, muddy peat, and then to overlying fibrous peat of buried soil B (Figs. 6 and 7). We sampled grain size every centimeter over the core depth interval 126.5–113.5 cm (Fig. 7).

Grain-size results show that for depths 126.5 cm up to 120.0 cm, the D50 grain size is very fine sand (60–100 μm). Then, there is an abrupt decrease in D50 grain size at 120 cm depth to a silt unit (20–60 μm), and the silt unit persists to the top of the 13 cm sample interval (113.5 cm depth). The differential volume plots of grain-size distributions (Fig. 7) show that for 2.5 cm immediately above the top of the buried soil (126.5–124 cm depth), the grain size coarsens upward slightly (all within the very fine sand range) and then slightly fines upward to 120.5 cm depth. Above 120.5 cm depth, the D50 of the deposit becomes notably finer, with an increase in silt at the expense of very fine sand (Fig. 7). At the coarsest end, there is a second minor peak in grain size (Fig. 8) at ~550 μm that is unaffected by change in depth above the buried soil; mica flecks are visible to the naked eye in the deposit and possibly may be the origin of this second minor peak in grain size.

For comparison, we also obtained grab samples for grain size from the modern tidal flat, which is 100–200 m southwest of the Sallys Bend core site. The D50 of the tidal flat is 115 μm (Fig. 6), a bit finer than the very fine sand–fine sand break. Compared to the samples from the core, the modern tidal flat has a peak grain size approximately equivalent to the grain-size peak for the silty very fine sand at 126.5 cm depth immediately above the buried soil (Fig. 8). However, the grain size for the modern tide flat is more heavily weighted, volume-wise, to the fine sand fraction at the expense of a smaller volume of silt (Fig. 8).

Companion foraminiferal analyses (Fig. 7) indicate that the very fine sand deposit directly above the buried soil contains a monospecific assemblage of *Miliammina fusca*, a common tidal flat and low marsh species (samples at 126–127 and 123–124 cm depth; Fig. 7). *M. fusca* was abundant (>50 individuals per sample), coarse grained, and included a range of sizes indicating juveniles and adults. The *M. fusca* specimens were largely intact and not fragmented. Three samples, positioned further up core at 121–122 cm, 120–121 cm, and 119–120 cm depths, had low abundances of foraminifera (<15 individuals per sample), contained only a few lone agglutinated foraminifera, and included one abraded calcareous foraminifera of the genus *Elphidiella* that has a marine affinity. Then, starting at 117–118 cm depth, which is 11 cm above the top of buried soil C, the silt-clay deposit contains abundant foraminifera typical of the upper part of the low marsh and low marsh–high transition (*Haplophragmoides wilberti*, *Jadammina macrescens*, *Trochammina inflata*). A similar assemblage is found at 113–114 cm depth before grading into a highest marsh environment at 110 cm depth, as indi-

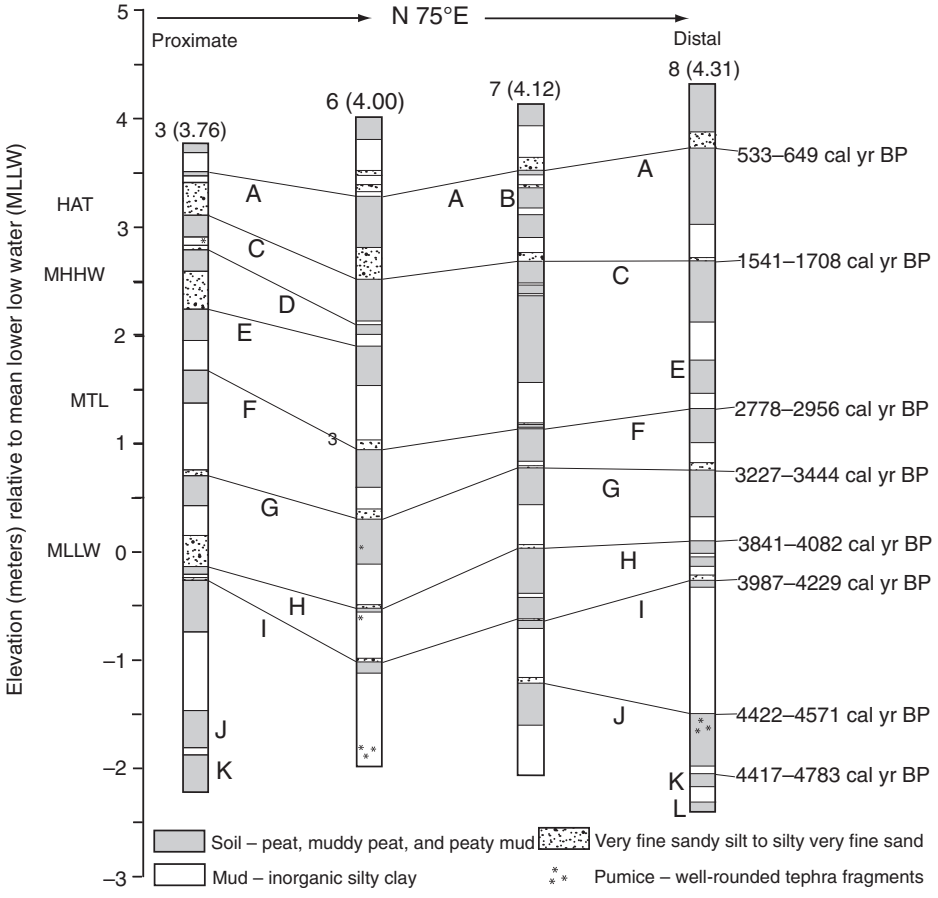

Figure 4. Lithostratigraphy of four cores along a N75°E transect. Total length of transect is 90 m. Cores are approximately evenly spaced (Fig. 3A). Parenthesized numbers that follow the core site number are elevations of individual core sites, accurate to nearest cm. The radiocarbon ages are for buried soils in core 8, expressed as calibrated age ranges at two standard deviations (Table 2). The soils were buried shortly after the indicated calibrated age, see text. Tidal datums recorded at South Beach, Oregon, tide gauge 9435380 (NOAA-COOPS, 2012): MTL—mean tidal level; MHHW—mean higher high water; HAT—highest astronomical tide as recorded at gauge on 31 December 1986. "Proximate" and "distal" indicate the location of the cores relative to the neighboring tidal flat.

cated by >50% *Trochamminita irregularis* (e.g., Engelhart et al., 2013a).

Diatoms were sampled between 108 and 138 cm in core 11, encompassing buried soil C, overlying clastic units, and the next-youngest fibrous peat, which is buried soil B. Based on rare freshwater or remnant estuarine valves in buried soil C at 138 and 129 cm (Figs. 6 and 7), the lower peat likely accumulated in a moist, freshwater upland environment. In contrast, the diatoms in the capping sandy deposit (samples 127, 126, and 124 cm; Figs. 5 and 6) dominantly consist of small, well-preserved tidal flat taxa. Greater than 80% of the diatom assemblage at 127, 126, and 124 cm consists of tidal flat diatom assemblages also identified by Riznyk (1973) in modern Yaquina Bay tidal flat deposits. In contrast, poorly preserved diatoms in overlying mud at 119 cm consist of a mix of muddy tidal flat, low marsh, and high marsh taxa (Figs. 6 and 7), suggesting a slower depositional rate and an environment transitional between low marsh and tidal flat. Diatoms in the peaty mud at 111 cm are consistent with accumulation in a high marsh (Fig. 7) and include common high marsh taxa (especially *Cosmioneis pusilla* and *Pinnularia lagerstedtii*). Moderately good preservation at 111 cm depth (Fig. 6) reflects the dominant occurrences of sturdy, intact marsh diatoms. At 107 cm depth, the high marsh environment is replaced by a wet freshwater upland environment, based on dominant occurrences of delicate freshwater taxa (*Eunotia* spp., *Gomphonema* spp.) in the uppermost fibrous peat sample within buried soil B (Fig. 6). The types of diatoms observed in buried soil B at 107 cm are similar to those observed in a sample taken 30 cm below the ground surface at core site 11, suggesting the peat of buried soil B accumulated in a spruce swamp or bog that was comparable to the modern environment at the core site.

Diatom analyses were additionally completed across the stratigraphic interval of buried soil G and the overlying cover sediment (Fig. 9). The stratigraphy consists of fibrous peat overlain by ~5 cm of sandy silt that contains peat rip-up clasts, which is then sequentially overlain by mud, peaty mud, and then the fibrous peat of buried soil F (Fig. 9).

The lower part of the sampled interval documents the abrupt transition from peat to overlying sandy deposit. Rare remnant diatoms in the lower peat samples at 350 cm and 342 cm depth indicate upland conditions (Fig. 9), and the silty very fine sand to very fine sandy silt above the peat at 340 cm includes pieces of peat. Diatoms in the 340 cm sample consist primarily of well-preserved tidal flat taxa, but ~14% of the assemblage consists of poorly preserved freshwater taxa that originate from the peat rip-up clasts (Fig. 8). The next two sandy samples at 339 cm and 337 cm similarly contain well-preserved tidal flat taxa.

The stratigraphically higher part of the sampled interval starts with lower marsh diatom assemblages and transitions to high marsh assemblages. The mud at 335 cm depth contains diatoms typically found in low marshes or in muddy, quiet depositional environments approximately near mean lower high water (MLHW; Fig. 9). Diatoms in peaty mud at 329 cm consist of a mix of tidal flat taxa and common, but mostly poorly preserved, high marsh taxa (Fig. 9). This mixed assemblage may be the result of reworking near the edge of a developing marsh. The uppermost sample in peat at 323 cm contains well-preserved high marsh taxa (Fig. 9), indicting redevelopment of a brackish marsh and development of the next highest soil, which is soil F.

Radiocarbon Ages

We used radiocarbon ages to determine the time of burial of a soil. Nine buried soils were dated using a total of 15 radiocarbon samples. Twelve ages came from core 8, and three ages came from core 11 (Table 2). For sample material, we used only detrital fragments that were delicate and identifiable (Table 2). The radiocarbon age was intended to give closely limiting maximum ages for time of soil burial; in the case of multiple ages for a single soil, the youngest age gives the most closely limiting maximum age for time of soil burial.

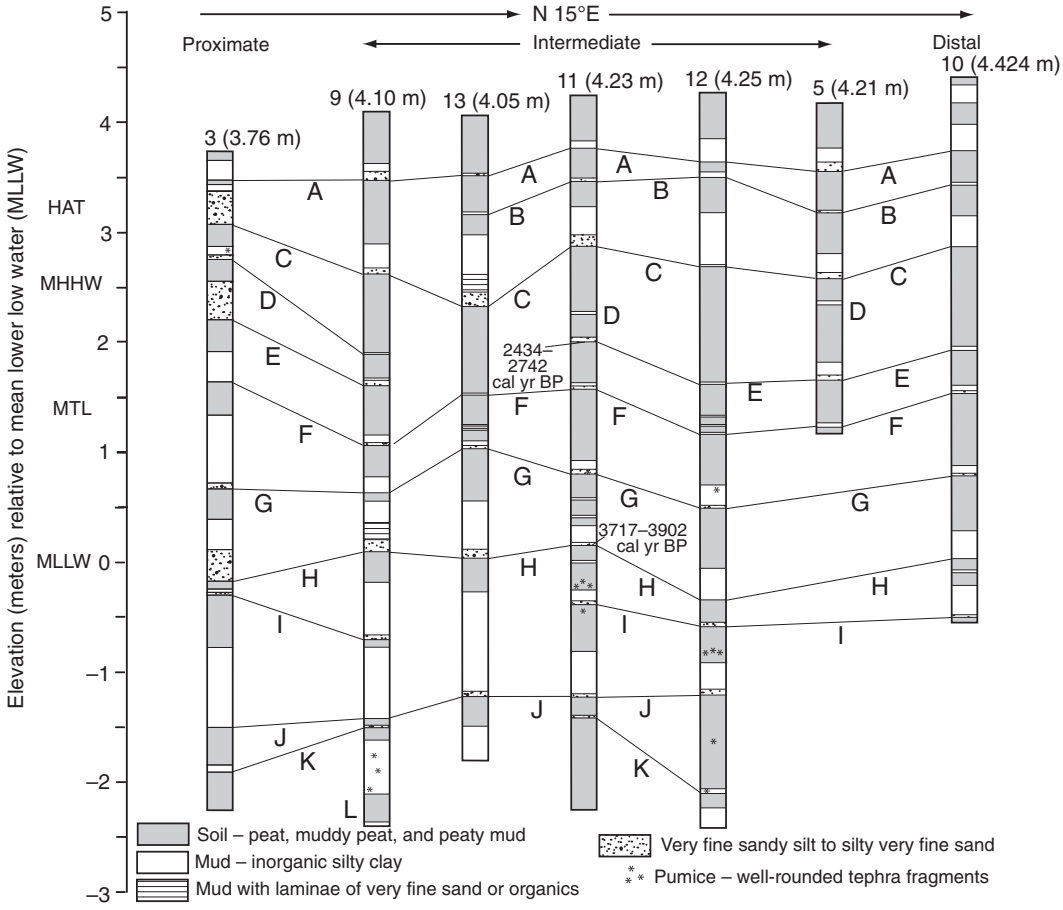

Figure 5. Lithostratigraphy of seven cores along a N15°E transect. Total length of transect is 100 m. Cores 3 9, 12, and 10 are on the transect, and the other three cores are <20 m off transect and were projected perpendicularly onto the transect line (Fig. 3A). Parenthesized numbers that follow the core site number are elevations of individual core sites, accurate to nearest cm. The radiocarbon ages are for buried soils in core 11, expressed as calibrated age ranges at two standard deviations (Table 2). The soils were buried shortly after the indicated calibrated age, see text. Tidal datums recorded at South Beach, Oregon, tide gauge 9435380 (NOAA-COOPS, 2012): MTL—mean tidal level; MHHW—mean higher high water; HAT—highest astronomical tide as recorded at gauge on 31 December 1986. "Proximate," "intermediate," and "distal" indicate the location of the cores relative to the neighboring tidal flat.

We address the question of how much older could the age be than a closely limiting maximum age by looking at soil in-built ages (Gavin, 2001). A radiocarbon age represents the time since carbon was removed from the atmosphere and incorporated in the sample measured. However, the sample had a finite age before it was incorporated, in turn, into the buried soil; that finite age is the in-built age (Gavin, 2001). The ideal situation would be a seed that fell from a plant onto the forest floor immediately before soil burial. In this best-case scenario, the calibrated age range of the detrital seed fragment gives a closely limiting maximum age for soil burial.

Based on the in-built age, delicate detritus used in dating the Sallys Bend buried soils could produce ages 50–250 yr older than a closely limiting maximum age. Individual calibrated age ranges (two standard deviations) in most cases are 100–200 yr (Table 2). With multiple age determinations for a single soil (e.g., soils G, H, I, and J; Table 2), the cumulative calibrated age range of multiple sample ages is 250–350 yr. Therefore, using the youngest calibrated sample range among multiple samples reduces the in-built age by as little as 50 yr (250 minus 200) or as much as 250 yr (350 minus 100). Conversely, maximum limiting age could be up to 300 yr older than the closely limiting maximum age of soil burial if one uses just a single age determination. Considering these inherent uncertainties in dating, a buried soil can date an earthquake only to the extent that the soil may provide a calibrated age range that is shortly before the earthquake occurred.

DISCUSSION

In the following, we discuss interpretations based on important observations in this study. Ten cores document the occurrence of 12 buried soils, of which the uppermost 10 buried soils are represented in most cores. Sandy deposits overlie most buried soils, and the sandy deposits thin inland from the tidal flat to Sallys Bend marsh and swamp. Based on grain size and microfossil analyses in two cores, the sandy unit is texturally a silty fine sand, similar to the texture of the adjacent tidal flat, and the fine sand abruptly transitions upward to mud. The fine sand unit has well-preserved diatoms and foraminifera of tidal flat affinity, whereas the overlying mud has diatoms and foraminifera of low marsh affinity. Nine buried soils have radiocarbon age determinations on samples consisting of delicate forest floor detritus from the top of the buried soil that range from ca. 4600 cal. yr B.P. to 600 cal. yr B.P. The calibrated age ranges are closely limiting maximum ages; that is, the age ranges represent times shortly before (50–300 yr before) soil burial.

Subduction Zone Earthquake History on the Central Oregon Coast

Submergence events that are abrupt in timing, long lasting, and documented in multiple cores at Sallys Bend are the best candidates for coseismic subsidence events caused by a Cascadia subduction zone earthquake (Nelson et al., 1996b). The eight buried soils that best meet these criteria are buried soils A, C, E, F, G, H, I, and J. For these buried soils, in most cases, the intervening mud thickness between adjacent buried soils is at least 10 cm thick (Table 3). Finally, buried soils C and G show biostratigraphic evidence of an abrupt change in salinity accompanying subsidence, based on diatom and foraminiferal data.

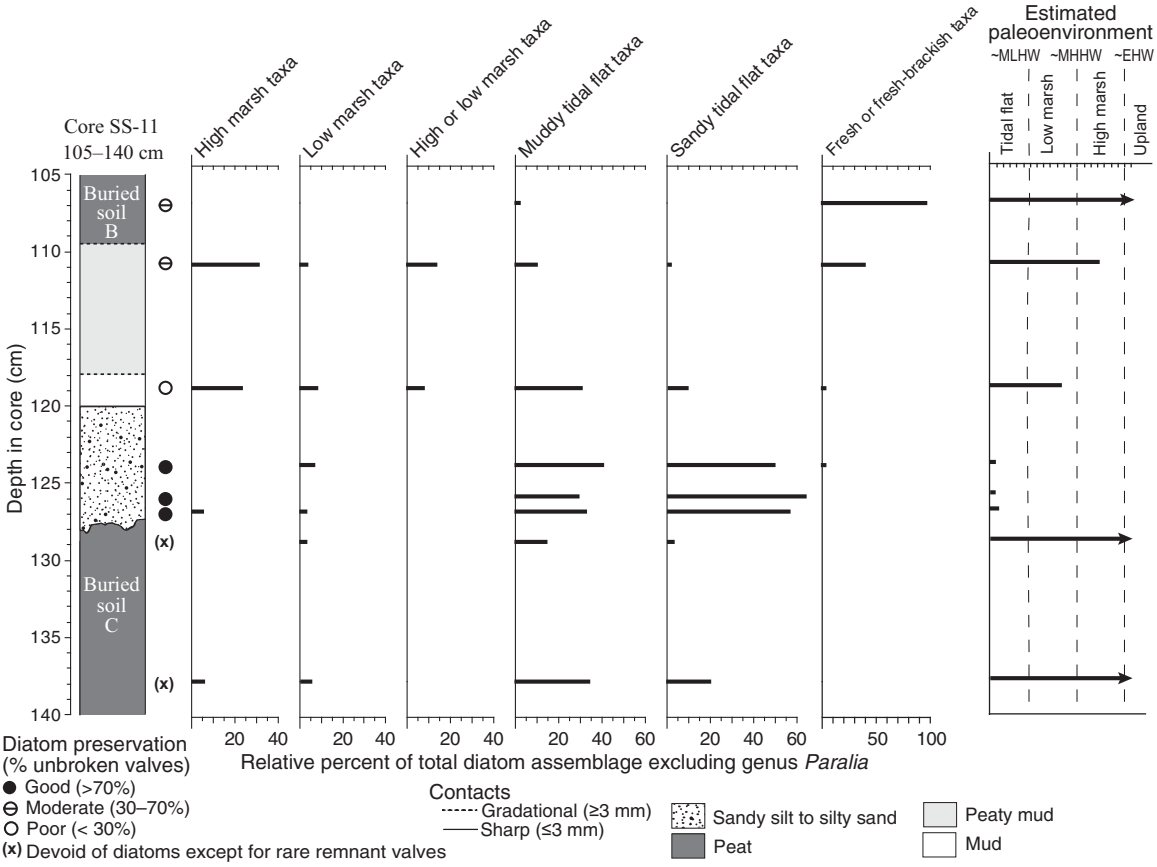

Figure 6. Diatom assemblage counts, diatom preservation, and inferred paleoenvironments for diatom assemblages, core 11, depth interval 105–140 cm. Tidal datums: MLHW—mean lower high water; MHHW—mean higher high water; EHW—extreme high water.

In addition, buried soils A, C, E, F, G, H, and I are widespread in the estuary, occurring along at least a 20 km reach of the estuary. The correlation of buried soils at Sallys Bend with buried soils 20 km up estuary is based on similarity in reported radiocarbon ages for buried soils at Sallys Bend with reported ages for buried soils at the Slack1 and OC-A core sites of Darienzo et al. (1994) (Figs. 2A and 10).

Two other buried soils, soils B and D, are documented in multiple cores, have abrupt upper contacts, and usually are overlain by a sandy unit (Figs. 4 and 5; Table 3), and each soil may be a signature of a subduction zone earthquake. However, these two buried soils do not usually have >10 cm of mud overlying them (Figs. 4 and 5), and therefore it is possible but inconclusive that soils B and D were buried as a consequence of a long-lasting submergence event. Other processes in addition to coseismic subsidence that could have produced soil burial for soils B and D include unusual floods or short-term elevated relative sea levels induced by oceanographic conditions (Nelson et al., 1996b).

Origin of Sandy Deposits on Top of Buried Soils

Constraints on Origin

Sandy deposits on top of buried soils have several characteristics that help constrain their origin. The sandy deposits decrease in thickness from the tidal flat edge inland (Figs. 4 and 5). The deposits are graded because the silty very fine sand to very fine sandy silt grades up section to muds (silt and clay) with no sand. The sandy deposits have foraminifera and diatom assemblages with tidal flat affinities (Fig. 7). Finally, in one sample near the top of the sandy deposit overlying soil C, there was a foraminiferal test of marine origin.

We infer that the process that produced the sandy deposits on top of soils C and G is the process responsible for the ubiquitous sandy deposits on top of every buried soil. The regularity of these sandy deposits overlying buried soils (Figs. 4 and 5) argues for a mechanism that happens every time a subduction zone earthquake occurs.

Tsunami as the Depositional Mechanism

One candidate mechanism to account for sandy deposits on top of buried soils is tsunami. Tsunamis accompany periodic subduction zone earthquakes, and these tsunamis leave characteristic deposits immediately on top of coseismically buried soils (Darienzo et al., 1994; Peterson and Priest, 1995; Kelsey et al., 2002; Witter et al., 2003; Nelson et al., 2004, 2008). However, did a tsunami lay down the diagnostic sandy deposit overlying buried soils at the Sallys Bend site, or was the deposit caused by another mechanism also related to a subduction earthquake?

River Flooding as the Depositional Mechanism

Coseismic shaking during earthquakes produces widespread landsliding, and the sediment products are transported to sites downstream (Hovius et al., 2011; Parker et al., 2011). Specifically in the case of the Yaquina River basin, widespread seismically induced slope failures could deliver sediment to channels, and, ulti-

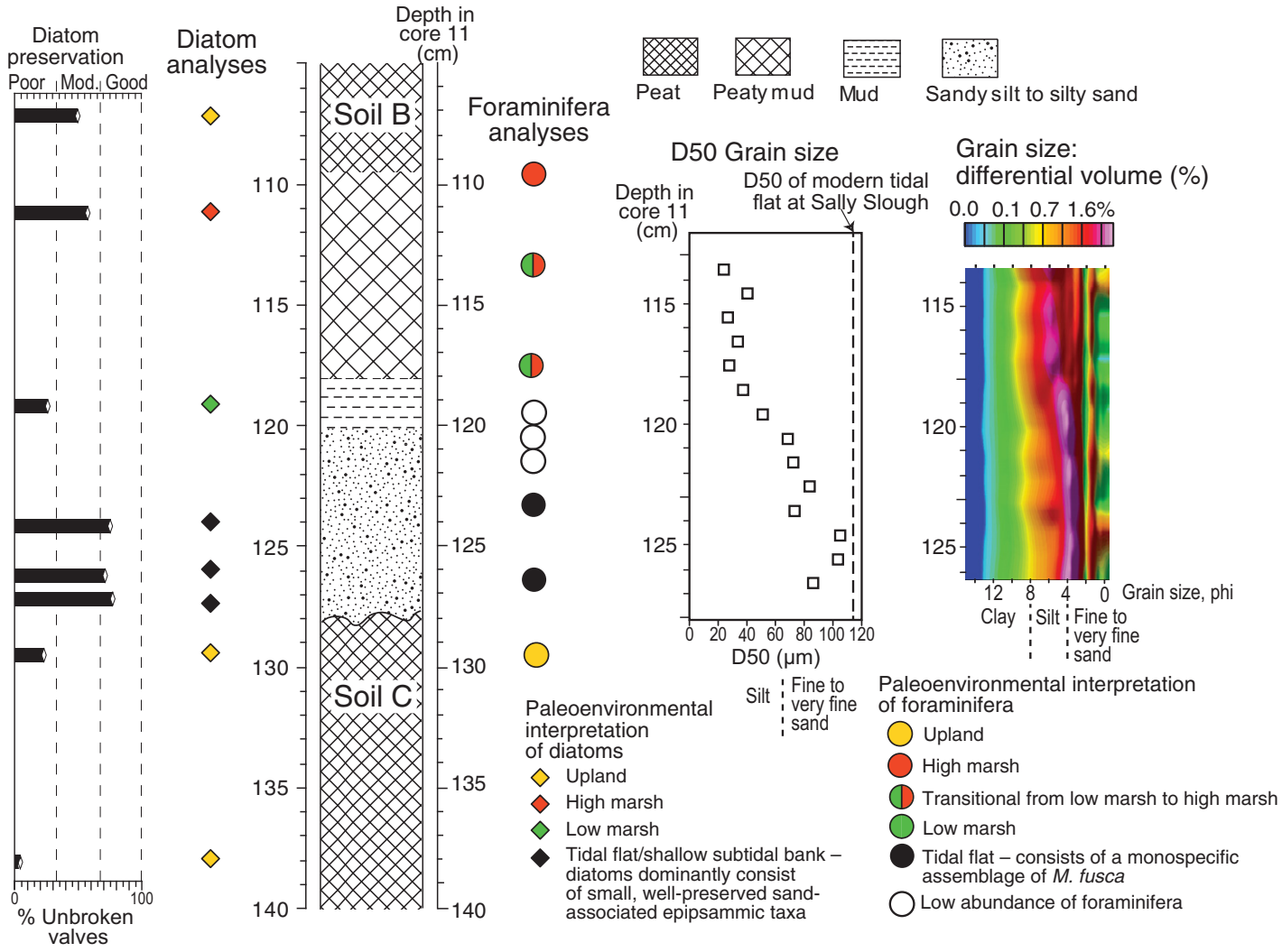

Figure 7. Biostratigraphic and grain-size analyses for buried soil C and overlying sediment. Samples were taken from core 11 (Figs. 3A, 5, and 6). Grain-size data are depicted both by median grain size (D50) vs. core depth and by differential volume vs. core depth. Differential volume is the percentage of total volume that each size class occupies. For each diatom sample and each foraminiferal sample, the length of the diamond symbol and the diameter of the circle symbol, respectively, correspond to the thickness of the core sampled.

mately, part of this sediment would be delivered as suspended fine sand to the lower reaches of the river during subsequent high discharges. The fluvial response to a subduction zone earthquake could include pulses of fine sand in suspension coming down to the estuary, through multiple tidal cycles, which remain as identifiable sediment packets in tidal marsh stratigraphy. Alternatively, multiple estuarine transport processes, driven by tides, wind fetch, and seasonal changes in sediment flux, mute out and dilute any coherent upstream signal that initially, upstream of the head of tide, was a pulse of fine sand in suspension.

Stratigraphic observations do not support a river-flooding origin for the sandy deposits on top of buried soils. Core observations in this and previous studies at Yaquina Bay (Darienzo and Peterson, 1995; Peterson and Priest, 1995; Data Repository [see footnote 1]) do not document seaward thinning of sand sheets deposited on paleo–tidal marshes, nor do Yaquina Bay tidal marshes display any sandy sedimentary structures typical of paleoflood deposits or have topographic settings where backwater flood deposits could accumulate (e.g., Benito and O'Connor, 2013). In addition, fine sand deposits on bay-fringing marshes contain intertidal diatoms and foraminifera but no freshwater diatoms.

In the Yaquina River estuary, the tidal flat setting also is an unlikely setting for deposition of primary flood deposits. The 50:1 ratio of tidal versus river discharge in the Yaquina Bay estuary (Peterson et al., 1984; Peterson and Priest, 1995) is consistent with the inference, from microfossil presence, that fine sand is reworked in the estuary. Also, based on work on tidal flats in Willapa Bay, Washington, situated in a setting similar to Yaquina Bay (Boldt et al., 2013), fluvial sediment deposited in tidal flats is highly susceptible to seasonal reworking by tidal currents.

Tsunami Signature: Deposition of Well-Preserved Intertidal Microfossils in a Low Marsh

In Sallys Bend marsh and swamp, the distinctive sandy deposits on top of buried soils have well-preserved diatoms and foraminifera with tidal flat affinity. The well-preserved character of the microfossils suggests that they were not deposited on a tidal flat and subject to reworking

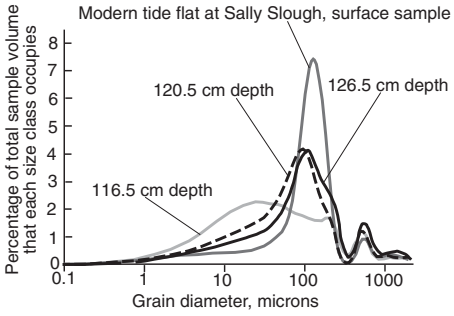

Figure 8. Comparative differential volume plots: tide flat surface sample vs. cover sediment above buried soil C in the adjacent Sallys Bend swamp and marsh. Depth 126.5 cm, 1 cm above buried soil and within sandy unit. Depth 120.5 cm, 7 cm above buried soil and within sandy unit. Depth 116.5 cm, 11 cm above buried soil and 3 cm above top of sandy unit that overlies buried soil.

by tidal currents. Rather the sandy deposits were deposited in a low marsh setting sufficiently high so that reworking by tidal currents was unlikely. If this inference is correct, the postsubsidence environment of these buried soils was low marsh rather than tidal flat. Also, the diatom and foraminifera with tidal flat affinity are not in situ assemblages but must have been transported in suspension to the low marsh environment. A tsunami is the only reasonable transporting flow because only a tsunami satisfies the condition that the flow must immediately follow abrupt submergence of the soil.

The observation that the sediment containing *M. fusca* has the same D50 as the tidal flat but is, overall, muddier than the tidal flat (compare differential volume distributions for tidal flat vs. sediment at 126.5 cm core depth; Fig. 8) is consistent with tsunami picking up sediment from the proximal sandy tidal flat close to the core sites. A tsunami origin for the deposit containing *M. fusca* also is supported by an absence of *M. fusca* incorporated into the underlying upland soil. Such an absence indicates rapid capping that would prevent sediment mixing (Engelhart et al., 2013b).

Also consistent with the inference that the intertidal foraminifera in the depth interval 128–199 cm (Fig. 7) were transported is the concurrent occurrence, at interval 121–122 cm, of an abraded calcareous foraminifera of the genus *Elphidiella* that, although too abraded to be identified at the species level, is nonetheless of marine origin. A recent study from Puget Sound, Washington, found that *Elphidiella hannai* occurred at a weighted average depth of 31.7 m (Martin et al., 2013), which supports an earlier study of the foraminifera on the central Oregon shelf that suggests a depth range of 17–50 m (Boettcher, 1967). *Elphidiella hannai* have also been reported in the main tidal channel at Yaquina Bay (e.g., Manske, 1968) and Netarts Bay (Hunger, 1966).

The overall good preservation of epipsammic (sand-associated) diatom taxa at Sallys Bend marsh and swamp also is consistent with entrainment by tsunami and subsequent falling out of suspension followed by rapid burial. Well-preserved epipsammic taxa occur in modern tsunami deposits (Kokociński et al., 2009; Sawai et al., 2009) as well as in paleotsunami deposits (Hemphill-Haley, 1995, 1996; Nanayama et al., 2007; Witter et al., 2009). The A.D. 1700 tsunami deposit at the Niawiakum River in Willapa Bay, Washington (USA), contains well-preserved tidal flat diatoms, the source of which is the extensive tidal flat between the mouth of Willapa Bay and the eastern shore of the estuary (Hemphill-Haley, 1995, 1996).

From a sedimentologic standpoint, the sandy deposits overlying buried soils are consistent with tsunami deposition. Tsunamis produce waves with long periods from 100 s to over 2000 s (Satake, 2002). The 7.5-cm-thick cover sediment above buried soil C consists of very fine sand on an eroded contact and rapidly transitions upward at 120 cm to mud (Fig. 6). Similarly, a distinct 4-cm-thick sandy unit with peat rip-up clasts occurs on an eroded contact above buried soil G (Fig. 8). Both observations are consistent with an erosive wavefront that entrains ripped up clasts of peaty soil and conveys water against rising topography to the north of Sallys Bend marsh and swamp (Fig. 2). Given the long period between waves, elevated water levels temporarily stagnate and provide a setting for the settlement out of suspension of entrained sand and unabraded foraminifera and diatoms, before the wave retreats oceanward.

Estimates of Amount of Coseismic Subsidence in Yaquina Bay during Subduction Zone Earthquakes

Diatom and foraminiferal analyses across the upper contact of buried soil C allow minimum estimates of 0.4–0.6 m for the coseismic subsidence that accompanied the subduction zone earthquake that occurred shortly after 1541–1708 cal. yr B.P.; a similar minimum estimate of coseismic subsidence, but an estimate based exclusively on diatoms, applies to the subduction zone earthquake that occasioned burial of soil G, which occurred shortly after 3227–3444 cal. yr B.P. Both soils C and G were developing in an upland environment at the time of coseismic subsidence, as indicated by freshwater diatoms and further supported for soil C by an absence of foraminifera.

For the earthquake that shortly followed 1541–1708 cal. yr B.P., soil C subsided a minimum of 0.4 m based on foraminiferal assemblages. The pre-earthquake elevation of soil C, relative to the tidal datum of MLLW, is unknown and can only be constrained at the lower-elevation end. Because buried soil C does not contain foraminifera, buried soil C could have developed at a minimum of 0.4 m above mean higher high water (MHHW), which is the highest elevation that foraminifera are found in transects of modern marshes in coastal Oregon (Hawkes et al., 2011; Engelhart et al., 2013a). Modern MHHW in Yaquina Bay is 2.54 m above MLLW (tide station 94335380; NOAA-COOPS, 2012) (Fig. 11). The lowest-elevation foraminifera not transported to the site by tsunami after coseismic subsidence are assemblages dominated by *Haplophragmoides wilberti, Jadammina macrescens*, and *Trochammina inflata*, which coupled with the absence of *M. fusca*, occur at elevations spanning from the upper portion of the low marsh to the low marsh–high marsh transition (mean high water [MHW] to MHHW; Fig. 11). Therefore, the highest elevation that foraminifera can live is 0.4 m above MHHW, and the most likely upper elevation that a post-coseismic subsidence foraminiferal assemblage will occupy is at MHHW; consequently soil C subsided a minimum of 0.4 m at the time of the earthquake that shortly followed 1541–1708 cal. yr B.P.

Similarly, based on diatom assemblages, coseismic subsidence of soil C and soil G was, at a minimum, 0.4 m. Rare remnant diatoms that are characteristically present in upland soils give way stratigraphically upward, across the upper buried soil contacts for soil C and soil G, to tidal flat diatoms in a sandy deposit (Figs. 6, 7, and 9). As discussed already, the overlying sandy deposit was transported to Sallys Bend by tsunami. The tsunami deposits that we infer overlie both soils C and G in turn give way stratigraphically upward to mud containing low marsh diatoms, which constitute the first in situ diatom assemblage after the earthquake (Figs. 6, 7, and 9). Therefore, tectonic subsidence dropped the site from upland elevations to low marsh conditions. Based on multiple transects in southern and central Oregon, the minimum upland elevation is ~0.4–0.6 m higher than the maximum low marsh elevation (Nelson and Kashima, 1993) (Fig. 11). Similarly, a modern transect at Alsea Bay, 21 km south of Yaquina Bay, shows that the upper-elevation limit of the low marsh is ~0.4–0.6 m lower than the lower-elevation limit of the upland–high marsh transition (Nelson et al., 2008). Therefore, based on diatom presence/absence, coseismic subsidence of soil C was, at a minimum, 0.4 m. The same

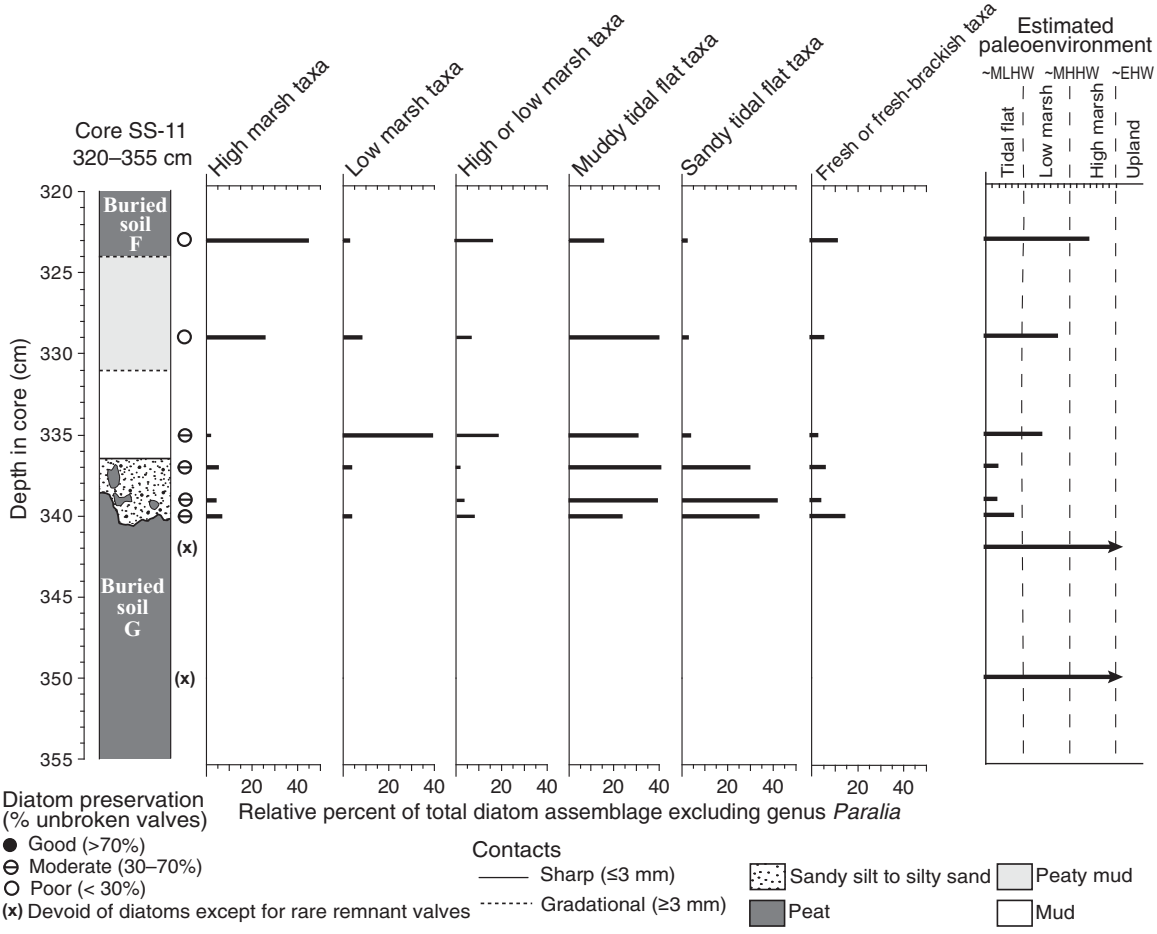

Figure 9. Diatom assemblage counts, diatom preservation and inferred paleoenvironments for diatom assemblages, core 11, depth interval 323–350 cm. Tidal datums: MLHW—mean lower high water; MHHW—mean higher high water; EHW—extreme high water.

case can be made in regards to the diatom biostratigraphy for buried soil G (Fig. 9), and we infer that coseismic subsidence of soil G was, at a minimum, 0.4 m.

Salt marsh diatoms and foraminifera will live up to the same elevation, and therefore, combining the results, we infer that minimum estimates for coseismic subsidence of soil C and soil G are 0.4–0.6 m. It is possible that coseismic subsidence was considerably greater because an upland forest environment, which was the environment of both buried soils C and G prior to burial, is too high to host foraminifera. Also, in the case of diatoms, buried soils C and G contained rare remnant diatoms characteristically present in upland soils at elevations as much as 1 m or more higher than maximum low marsh elevation diatoms. Furthermore, detritus in soils C and G included spruce needles and small branches (<1.5 mm diameter) typical of an upland forest floor setting.

The next estuary to the south (Alsea Bay, 18.5 km south) has evidence for a subduction zone earthquake at ca. 1.6 ka. Transfer function analyses of foraminifera assemblages across the 1.6 ka buried soil contact at Alsea Bay yield a range of coseismic subsidence estimates from 0.09 ± 0.20 m to 0.46 ± 0.12 m (Nelson et al., 2008); the range of coseismic subsidence estimates is either approximately the same or substantially less than the minimum amount of coseismic subsidence estimated for Yaquina Bay shortly after 1541–1708 cal. yr B.P., which is 0.4 m.

Preservation of Buried Soils and the Completeness of the Record of Past Earthquakes

During a subduction zone earthquake cycle, tidal deposition and coastal wetland soil development precedes subsequent soil burial, and preservation of a soil that coseismically subsides requires that the site be submerged long enough to accumulate a tidal mud layer (Atwater and Hemphill-Haley, 1997; Atwater, 1997). Multiple, stacked buried soils collectively can chronicle a series of plate-boundary earthquakes if persistent, long-term relative sea-level rise, only interrupted by brief periods of coseismic subsidence, takes place. Long-term relative sea-level rise, persisting through the duration of a plate-boundary seismic cycle (hundreds of years to a millennium), provides accommodation space for deposition of mud after soil subsidence. Not all coseismically buried soils are well preserved under conditions of long-term relative sea-level rise because an instance of relatively small coseismic subsidence could result in a weakly preserved buried soil. For instance, in the context of long-term relative sea-level rise, Cascadia paleoseismic sites display sequences that consist of both strongly preserved and weakly preserved buried soils (Atwater and Hemphill-Haley, 1997; Kelsey et al., 2002; Witter et al., 2003; Nelson et al., 2008).

In order to use the Sallys Bend buried soils sequence to estimate the average recurrence interval for earthquakes, the buried soil sequence should be complete. If, over time, the

TABLE 2. RADIOCARBON RESULTS FROM SALLYS BEND, YAQUINA BAY

Buried soil	Sample no.*	Sample interval† (cm)	Material dated	Lab no.§	$\delta^{13}C$# (‰)	^{14}C yr B.P.§	Age** (cal yr B.P.)
A	SS8 68	68–70	Seeds	297827	–25.9	580 ± 30	533–569, 582–649
C	SS8 154.5	154.5–155.5	3 twigs w/branch nodes	287388	–26.0	1710 ± 40	1541–1708
E	SS11 223	220–223	Spruce cone	287392	–25.2	2500 ± 40	2434–2742
F	SS8 304	304–305	Wood, bark, 2 seed pods	287389	–30.4	2770 ± 40	2778–2956
G	SS8A 358B	358–359	Wood w/branch node	287391	–25.4	3210 ± 40	3361–3510, 3531–3556
G	SS8A 358A	358–359	Needles	287390	–27.2	3120 ± 40	3227–3408, 3425–3444††
H	SS8 420	420–421	Needles & seeds	297828	–25.0	3630 ± 40	3841–4009, 4030–4082
H	SS11 412.5	412.5–413.5	Needles & seeds	296064	–25.5	3580 ± 30	3777–3788, 3827–3976
H	SS11B 415	415–416	Needles	296065	–25.9	3540 ± 30	3717–3902††
I	SS8A 457.5A	457.5–458.5	Needles	296060	–26.5	3750 ± 30	3987–4048, 4065–4162, 4168–4180, 4198–4229††
I	SS8A 457.5B	457.5–458.5	Seeds & twigs	296061	–25.5	3800 ± 30	4088–4259, 4264–4287
J	SS8 564.5A	564.5–565.5	Seeds	297829	–26.9	4030 ± 40	4417–4588, 4593–4613, 4766–4783
J	SS8 564.5B	564.5–565.5	Needles	297830	–27.7	4180 ± 40	4582–4769, 4781–4838
J	SS8C 582.5	582.5–583.5	Needles & seeds	296062	–25.4	4030 ± 30	4422–4571††
K	SS8C 638	638–639	Needles, seed pod	296063	–25.8	4030 ± 40	4417–4588, 4593–4613, 4766–4783

*Sample number designates locality, core site number, and upper depth of sample.
†Numbers are depths from ground surface in centimeters. All samples are from uppermost 1 cm of buried soil, except SS-11-223, which was collected 3 cm above top of buried soil.
§Lab reported ages from Beta Analytic, Inc.
#Measured $^{13}C/^{12}C$ ratios ($\delta^{13}C$ relative to the Peedee belemnite [PDB-1] standard).
**Calibrated age ranges (two standard deviations) reported as yr B.P. (B.P.—before present), where "present" is A.D. 1950, using CALIB calibration version 7.0 program (Stuiver and Reimer, 1993) and IntCal13 data set (Reimer et al., 2013).
††Youngest calibrated age range selected from multiple dated samples for soil.

site emerges relative to sea level and becomes too high to subside into the tidal zone during subduction zone earthquakes, then such emergence marks the end of a potentially complete buried soil sequence.

Even though the A.D. 1700 earthquake and accompanying tsunami left evidence of tectonic subsidence and tsunami deposits at the adjacent estuaries of Siletz River, Salmon River, and Alsea Bay and at other sites within Yaquina Bay (including at core OC-A; Fig. 2A; Darienzo, 1991; Darienzo et al., 1994; Peterson and Priest, 1995; Nelson et al., 2004, 2008), the A.D. 1700 earthquake is not recorded at Sallys Bend (Fig. 3). In eight estuaries that span a range from southern to northern Oregon, transfer-function–based microfossil estimates of coseismic subsidence during the A.D. 1700 earthquake range from 0.20 to greater than 0.81 m (Wang et al., 2013). However, in A.D. 1700, the marsh and swamp at Sallys Bend were too high to record a similar amount of coseismic subsidence.

The modern elevation range of the surface of the spruce forest at the Sallys Bend site is 0.9–1.3 m higher than the top of the high marsh (Fig. 11). Today, in order for the Sallys Bend site to be submerged by coseismic subsidence during a subduction zone earthquake and convert a surface soil to a buried soil, the site would have to subside by more than 1.0 m. A similar condi-

TABLE 3. BURIED SOIL ATTRIBUTES CONSISTENT WITH SUBDUCTION EARTHQUAKE ORIGIN FOR SOIL BURIAL

Buried soil	Sharp (<3 mm) contact between buried soil and overlying mud	Long-lasting relative sea-level rise (overlying mud >10 cm thick)	Fine to very fine sand layer immediately overlies buried soil	Where available, diatom assemblages are consistent with abrupt relative sea-level rise accompanying soil burial*	The buried soil is laterally extensive, e.g., observed up estuary†	Calibrated age range (2σ) of buried soil is chronologically consistent with regional record of Cascadia subduction zone earthquakes§
A	X	X	X	na	X	X
B	X		X	na		
C	X	X	X	X	X	X
D	X		X	na		
E	X	X	X	na	X	X
F	X	X	X	na	X	X
G	X	X	X	X	X	X
H	X	X	X	na	X	X
I	X	X	X	na	X	X
J	X	X	X	na		X

*na—not available.
†Based on correlation of Sallys Bend ages and stratigraphy with up-estuary core stratigraphy and ages from sites Slack1 and OC-A of Darienzo et al. (1994) (Figs. 2A and 10).
§Regional records of Cascadia subduction zone earthquakes compiled in Nelson et al. (2006).

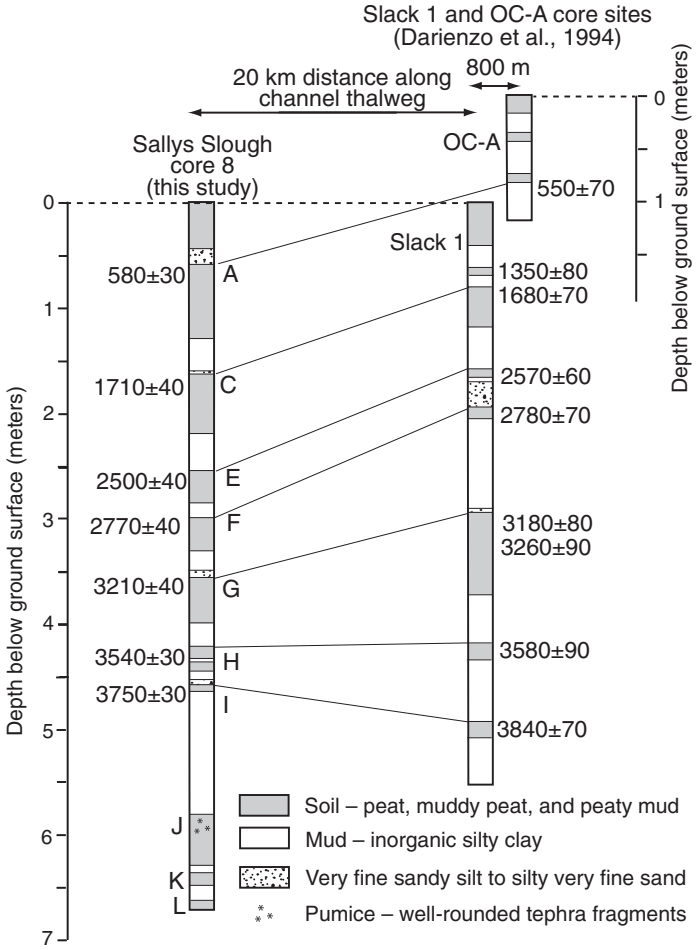

Figure 10. Correlation of Slack 1 and OC-A cores (Fig. 2A), which were logged by Darienzo et al. (1994), to Sallys Bend core 8 (Figs. 2B and 3A), which is 20 km downstream following the thalweg of the Yaquina Bay estuary. There is no elevation survey between Sallys Bend core 8 and the two cores 20 km upstream; for purposes of comparing the stratigraphy in the cores, the three cores are positioned by equating the core ground surface heights at core 8 and core Slack 1. Reported ages are in ^{14}C yr B.P. from Darienzo et al. (1994) for the Slack 1 and OC-A cores and from this study for core 8 (Table 2).

tion probably would have been the case in the recent past, i.e., in A.D. 1700. In 1914, topographers with the U.S. Coast and Geodetic Survey documented, at the location of the Sallys Bend core site, a distinct boundary between intertidal flat and marsh-swamp-forest upland (Fig. 3A). Despite subsequent development of road fill and roads (Fig. 3B), the same clearly defined boundary is apparent today.

Sometime after the burial of soil A, which was shortly after 533–649 cal. yr B.P., a change in site condition became apparent at Sallys Bend, as reflected in the youngest part the geologic record. Prior to that time, most buried soils are capped by at least a 10-cm-thick mud layer, indicating that ongoing relative sea-level rise provided the accommodation space to preserve each succeeding soil through burial. However, after burial of soil A, the relative sea-level trend shifted from rising to stasis or slightly falling. That is, shortly after the accumulation of >10 cm of mud on top of buried soil A, sea level no longer increased relative to the land surface. This shift accounts for the observations that today buried soil A is at or above highest astronomical tide (HAT), and buried soil C is at the approximate elevation of MHHW (Figs. 4 and 5). The stasis or slight fall in relative sea level also accounts for no preservation of the A.D. 1700 soil.

Other paleoseismic sites in coastal Oregon share the situation evident at Yaquina Bay, in which a single paleoseismic core site, such as Sallys Bend, ceases to be a recorder of paleoearthquakes, but other core localities in the same estuary have young buried soils that do record the most recent earthquake. For instance, on the Coquille River estuary, a paleoseismic core site named Sevenmile, with a 6700-yr-long record, does not record the youngest earthquake (i.e., A.D. 1700), but an adjacent core site, named Osprey, does record this earthquake (Witter et al., 2003) with a minimum subsidence of 0.81 m (Engelhart et al., 2013b). Similarly, the Sixes River meander bend site (Kelsey et al., 2002) has a 5500-yr-long paleoseismic history but does not record the A.D. 1700 earthquake, while a site at the mouth of the Sixes River, 2 km downstream, does record subsidence during the A.D. 1700 earthquake (Kelsey et al., 1998).

Average Recurrence Interval of Subduction Zone Earthquakes at Sallys Bend

Estimates of average earthquake recurrence consider the part of the buried soil record, from soil A to soil J, that we infer to have been buried by mud deposition during long-term rising relative sea level. Eight of 10 of these soils (A, C, E, F, G, H, I, and J) are well represented in multiple cores. The remaining two soils, as discussed earlier, may represent earthquakes but are not as well preserved and may represent other nontectonic processes. Soil B is preserved in 5 of 11 cores and is overlain by >10 cm of mud in only two cores. Soil D, although represented in 6 of 11 cores, has only a minimal overlying mud layer (Figs. 4 and 5). Therefore, we employ a minimum of seven and a maximum of nine intervals between earthquakes to allow for uncertainty in the number of earthquakes bracketed between well-preserved soil A and well-preserved soil J. Considering seven to nine interearthquake intervals over the time span of 3770–4040 yr (time span between maximum limiting ages of buried soils A and J, incorporating uncertainty in endpoint ages; Fig. 3; Table 2), the average recurrence interval of subduction zone earthquakes in the Sallys Bend marsh record, rounding to the nearest decade, is 420–580 yr. By way of contrast, Darienzo and Peterson (1995) estimated an average recurrence interval for Yaquina Bay, based on five interearthquake intervals, of 360–590 yr.

Addition of Sallys Bend to the Growing Archive of Paleoseismic Sites: Incremental Insights to Cascadia Rupture Behavior

The Sallys Bend paleoseismic record within Yaquina Bay spans >4000 yr and fills in a gap where, previously, there was no long record in central Oregon (Fig. 12). When placed in the

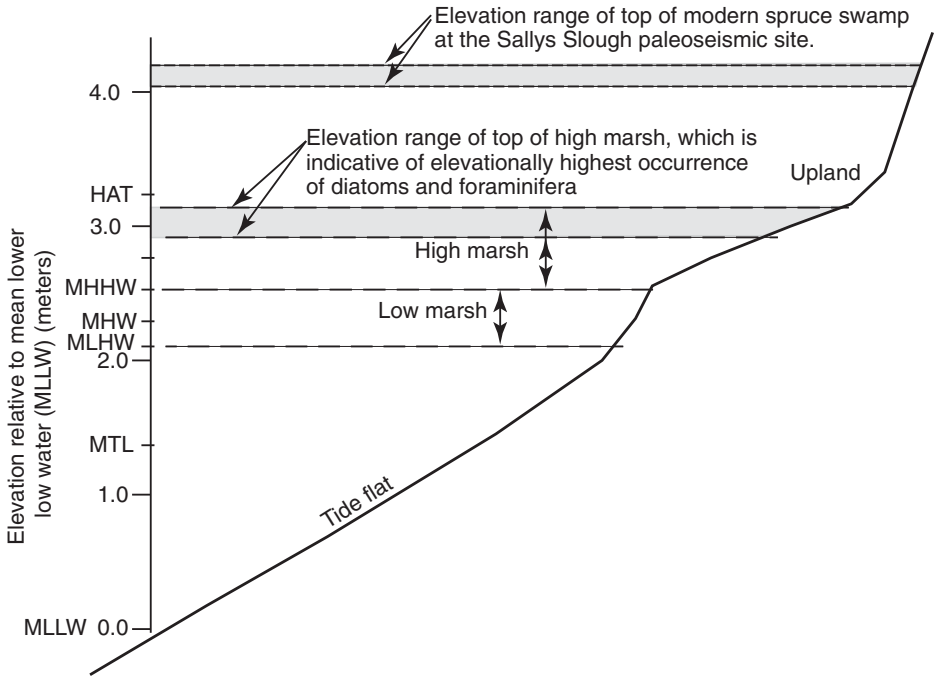

Figure 11. Intertidal zones defined by tidal flat, low marsh, high marsh, and upland. Topographic profile is schematic and is at a variable vertical exaggeration. Tide datums (elevations) are for National Oceanic and Atmospheric Administration (NOAA) station 9435380, South Beach, Oregon (NOAA-COOPS, 2012): MHHW—mean higher high water; MHW—mean high water, MLHW—mean lower high water; MTL—mean tidal level. The diurnal range of tide (difference in height between MHHW and MLLW) at tidal station 9435380 is 2.542 m. The tide-flat-to-low-marsh and low-marsh-to-high-marsh transitions, relative to tide datum, are from Hemphill-Haley (1995) and Nelson et al. (2008). Upland is assumed to be 0.6 m above the highest elevation of the low marsh, which places the high marsh–upland transition 0.15 m below the highest astronomical tide (HAT) as recorded at station 9435380 on 31 December 1986.

context of published paleoseismic records for the Cascadia subduction zone, the Sallys Bend record allows for long ruptures, serial ruptures, and shorter ruptures, because correlation among individual site chronologies is limited by the two-sigma calibrated radiocarbon age ranges and by the fact that the duration of complete records varies from site to site. Heaton and Hartzell (1987) posited, almost three decades ago, that these three rupture modes were possible at the Cascadia subduction zone based on historic earthquake behavior at other subduction zones.

Analysis of offshore turbidite records (Goldfinger et al., 2012, 2013) is another approach to addressing rupture mode at Cascadia. However, on-land paleoseismic site chronologies cannot test the inference, based on offshore turbidites records, of multiple long ruptures (Goldfinger et al., 2012). Because of dating uncertainty, on-land records both allow for long ruptures and also allow for serial ruptures that are closely spaced in time that sum to about the same length (e.g., Nelson et al., 1995).

The value of the on-land record is one of incremental additional information with each record. No one additional record is going to fully characterize a particular earthquake nor address how frequently, if ever, the whole subduction zone ruptures in a series of ruptures closely spaced in time. However, with incremental additions of paleoseismic information, temporal-spatial patterns of rupture from on-land sites emerge. Each incremental paleoseismic site aids in understanding the potential range of seismic behavior on the Cascadia subduction zone. Two examples follow.

An emerging observation, also apparent in a comparative compilation of Nelson et al. (2006), is that while northern coastal Oregon has recorded one or two earthquakes in the first half of the last millennium (500–1000 cal. yr B.P.), southern coastal Oregon sites recorded no or at most one subduction zone earthquake in the first half of the last millennium (Fig. 12). This in part may be a problem of incomplete recording, but neither Coquille estuary nor Bradley Lake, two sites in southern coastal Oregon, are sites for which an incomplete record is suspect for this 500–1000 cal. yr B.P. period (Witter et al., 2003; Kelsey et al., 2005).

Second, the earthquake that buried soil C at Sallys Bend, which occurred shortly after 1541–1708 cal. yr B.P., can be correlated within calibrated age ranges to an earthquake at eight other sites from, north to south, southwest Washington to Bradley Lake, but an earthquake within such an age range is not represented further south at Sixes River, which enters the Pacific Ocean at Cape Blanco (Fig. 12). An additional pertinent observation is that two tsunamis closely spaced in time (~22 yr apart; Kelsey et al., 2005) occurred at Bradley Lake (26 km north of Cape Blanco) shortly after 1600–1820 cal. yr B.P. One tsunami was bigger than the other, based on deposit thickness. These two tsunamis may represent two ruptures in serial, with the northern rupture extending from near Cape Blanco all the way north to at least southwest Washington, and a smaller rupture extending south from the vicinity of Cape Blanco, which involved too little slip to significantly subside the mouth of the Sixes River.

CONCLUSIONS

At Sallys Bend, Yaquina Bay, eight to 10 subduction zone earthquakes are recorded by buried soils that collectively span an age range from 533 to 4571 cal. yr B.P. In two cases, shortly after 1541–1708 cal. yr B.P. and shortly after 3227–3444 cal. yr B.P., the buried soils coseismically subsided by at least 0.4 m based on microfossils-based estimates of the amount of coseismic subsidence. Preservation of coseismically buried soils occurred until ~500–600 yr ago, after which preservation was compromised by cessation of gradual relative sea-level rise, which in turn precluded drowning of marsh soils during instances of coseismic subsidence. The average recurrence interval between earthquakes, for the 3770–4040 yr length of record, is 420–580 yr. This average recurrence interval incorporates uncertainty in the length of record derived from the two standard-deviation calibrated age range for earthquake timing and uncertainty in whether the number of interearthquake intervals is seven, eight, or nine. Sandy deposits on top of buried soils are of tsunamigenic origin because they fine upward, thin landward, and contain well-preserved, unreworked intertidal microfossils that were rapidly delivered to the tidal marsh from the estuary. The possibility that the sandy deposits were sourced directly from landslides triggered upstream in the Yaquina River basin by seismic shaking is discounted based on sedimentologic,

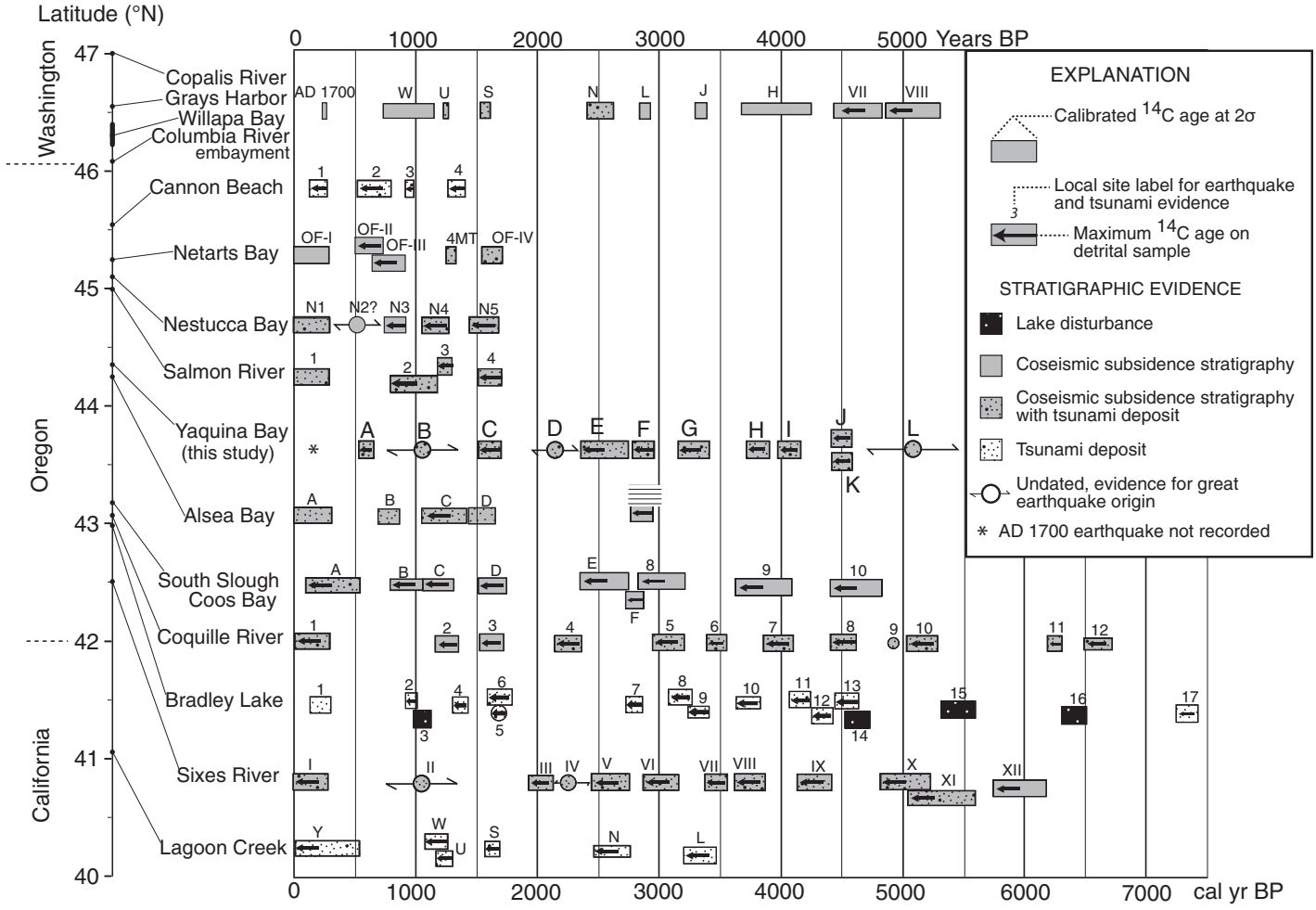

Figure 12. Subduction zone earthquake histories for individual paleoseismic investigation sites, plotted as a function of latitude (modified from Nelson et al., 2006). All investigation sites are located on Figure 1, and data sources for individual earthquake histories are specified in the Figure 1 caption. Rectangles delineate ages of inferred subduction zone earthquakes; widths of rectangles delineate the calibrated age range to two standard deviations. Alphanumeric code above the rectangle is the local site earthquake designation.

microfossil, and depositional site characteristics of the sandy deposits, which are inconsistent with a fluvial origin. Finally, the comparison of the Yaquina Bay earthquake record to other similar records at Cascadia coastal sites helps to define potential patterns of rupture for different earthquakes; however, inherent uncertainty in dating precludes definitive statements about rupture length during individual earthquakes.

ACKNOWLEDGMENTS

Graehl received funding from a Geological Society of America graduate student research grant. Engelhart's participation was supported by National Science Foundation grant EAR-0842728. The Oregon Department of Geology and Mineral Industries (DOGAMI) provided field equipment and funded the radiocarbon analyses. Jonathan Allan and Laura Stimely of the DOGAMI, Newport, Oregon, office provided scientific and logistical support and field assistance. George Priest, also of DOGAMI, provided insight to previous work and to the 1914 U.S. Coast and Geodetic Survey maps within the field area. Others who provided field assistance include Morgan Annable, Jody Stecher, Kyle French, and Heath Sawyer. Land access was provided by Cheryl Brown, Christopher Janousek, Jeff Ingram, Esther Lev, Laura Brophy, Matt Gehrenbacher, Don and Peggy Johnston, Pat at Mill Creek, the port of Toledo, and the city of Toledo. We are particularly grateful for land access to Sallys Bend provided by Mark and Joyce Lawrence. Jessica Pilarczyk constructed the grain-size differential volume plot in Figure 7 and assisted in identification of the abraded calcareous foraminifer. We thank Science Editor Hope Jahren for overseeing science review. Reviews by Brian Sherrod, Brian Atwater, Chris Goldfinger, and Associate Editor An Yin substantially improved the manuscript.

REFERENCES CITED

Abramson, H.A., 1998, Evidence for Tsunamis and Earthquakes during the last 3,500 Years from Lagoon Creek, a Coastal Freshwater Marsh, Northern California [M.S. thesis]: Arcata, California, Humboldt State University, 76 p.

Atwater, B.F., 1987, Evidence for great earthquakes along the outer coast of Washington State: Science, v. 236, p. 942–944, doi:10.1126/science.236.4804.942.

Atwater, B.F., 1997, Coastal Evidence for Great Earthquakes in Western Washington: U.S. Geological Survey Professional Paper 1560, p. 77–90.

Atwater, B.F., and Hemphill-Haley, E., 1997, Recurrence Intervals for Great Earthquakes of the Past 3500 Years at Northeastern Willapa Bay, Washington: U.S. Geological Survey Professional Paper 1576, 108 p.

Atwater, B.F., Tuttle, M.P., Schweig, E.S., Rubin, C.M., Yamaguchi, D.K., and Hemphill-Haley, E., 2004, Earthquake recurrence inferred from paleoseismology, *in* Gillespie, A.R., Porter, S.C., and Atwater, B.F., eds., The Quaternary Period in the United States: New York, Elsevier, p. 331–350.

Benito, G., and O'Connor, J.E., 2013, Quantitative paleoflood hydrology, *in* Shroder, J., and Wohl, E.E., eds., Treatise on Geomorphology, Volume 9, Fluvial Geomorphology: San Diego, California, Academic Press, p. 459–474.

Boettcher, R.S., 1967, Foraminiferal Trends of the Central Oregon shelf [M.S. thesis]: Corvallis, Oregon, Oregon State University, 143 p.

Boldt, K.V., Nittrouer, C.A., and Ogston, A.S., 2013, Seasonal transfer and net accumulation of fine sediment on a muddy tidal flat: Willapa Bay, Washington: Con-

tinental Shelf Research, v. 60, p. S157–S172, doi:10.1016/j.csr.2012.08.012.

Darienzo, M.E., 1991, Late Holocene Paleoseismicity along the Northern Oregon Coast [Ph.D. thesis]: Portland, Oregon, Portland State University, 176 p.

Darienzo, M.E., and Peterson, C.D., 1995, Magnitude and frequency of subduction zone earthquakes along the northern Oregon coast in the past 3000 years: Oregon Geology, v. 57, p. 3–12.

Darienzo, M.E., Peterson, C.D., and Clough, C., 1994, Stratigraphic evidence for great subduction-zone earthquakes at four estuaries in northern Oregon, U.S.A.: Journal of Coastal Research, v. 10, p. 850–876.

Engelhart, S.E., Horton, B.P., Vane, C.H., Nelson, A.R., Witter, R.C., Brody, S.R., and Hawkes, A.D., 2013a, Modern foraminifera, $\delta^{13}C$, and bulk geochemistry of central Oregon tidal marshes and their application in paleoseismology: Palaeogeography, Palaeoclimatology, Palaeoecology, v. 377, p. 13–27, doi:10.1016/j.palaeo.2013.02.032.

Engelhart, S.E., Horton, B.P., Nelson, A.R., Hawkes, A.D., Witter, R.C., Wang, K., Wang, P.-L., and Vane, C.H., 2013b, Testing the use of microfossils to reconstruct great earthquakes at Cascadia: Geology, v. 41, p. 1067–1070, doi:10.1130/G34544.1.

Garrison-Laney, C.E., 1998, Diatom Evidence for Tsunami Inundation from Lagoon Creek, a Coastal Fresh Water Pond, Del Norte County, California [M.S. thesis]: Arcata, California, Humboldt State University, 97 p.

Gavin, D.G., 2001, Estimation of inbuilt age in radiocarbon ages of soil charcoal for forest fire studies: Radiocarbon, v. 43, p. 27–44.

Goldfinger, C., Nelson, C.H., Morey, A.E., Johnson, J.E., Patton, J.R., Karabanov, E., Gutiérrez-Pastor, J., Eriksson, A.T., Gràcia, E., Dunhill, G., Enkin, R.J., Dallimore, A., and Vallier, T., 2012, Turbidite Event History—Methods and Implications for Holocene Paleoseismicity of the Cascadia Subduction Zone: U.S. Geological Survey Professional Paper 1661–F, 170 p. (Available at http://pubs.usgs.gov/pp/pp1661f/).

Goldfinger, C., Morey, A.E., Black, B., Beeson, J., Nelson, C.H., and Patton, J.R., 2013, Spatially limited mud turbidites on the Cascadia margin: Segmented earthquake ruptures?: Natural Hazards and Earth System Sciences, v. 13, p. 2109–2146, doi:10.5194/nhess-13-2109-2013.

Hawkes, A.D., Horton, B.P., Nelson, A.R., Vane, C.H., and Sawai, Y., 2011, Coastal subsidence in Oregon, USA, during the giant Cascadia earthquake of AD 1700: Quaternary Science Reviews, v. 30, p. 364–376, doi:10.1016/j.quascirev.2010.11.017.

Heaton, T.H., and Hartzell, S.H., 1987, Earthquake hazards on the Cascadia subduction zone: Science, v. 236, p. 162–168, doi:10.1126/science.236.4798.162.

Hemphill-Haley, E., 1995, Diatom evidence for earthquake-induced subsidence and tsunami 300 years ago in southern coastal Washington: Geological Society of America Bulletin, v. 107, p. 367–378, doi:10.1130/0016-7606(1995)107<0367:DEFEIS>2.3.CO;2.

Hemphill-Haley, E., 1996, Diatoms as an aid in identifying late Holocene tsunami deposits: The Holocene, v. 6, p. 439–448, doi:10.1177/095968369600600406.

Hovius, N., Meunier, P., Ching-Weei, L., Hongey, C., Yue-Gau, C., Dadson, S., Ming-Jame, H., and Lines, M., 2011, Prolonged seismically induced erosion and the mass balance of a large earthquake: Earth and Planetary Science Letters, v. 304, p. 347–355.

Hunger, A.A., 1966, Distribution of Foraminifera, Netarts Bay, Oregon [M.Sc. thesis]: Corvallis, Oregon, Oregon State University, 112 p.

Kelsey, H.M., Witter, R.C., and Hemphill-Haley, E., 1998, Response of a small Oregon estuary to coseismic subsidence and postseismic uplift in the past 300 years: Geology, v. 26, p. 231–234, doi:10.1130/0091-7613(1998)026<0231:ROASOE>2.3.CO;2.

Kelsey, H.M., Witter, R.C., and Hemphill-Haley, E., 2002, Plate-boundary earthquakes and tsunamis of the past 5500 years, Sixes River estuary, southern Oregon: Geological Society of America Bulletin, v. 114, p. 298–314, doi:10.1130/0016-7606(2002)114<0298:PBEATO>2.0.CO;2.

Kelsey, H.M., Nelson, A.R., Hemphill-Haley, E., and Witter, R.C., 2005, Tsunami history of an Oregon coastal lake reveals a 4600 yr record of great earthquakes on the Cascadia subduction zone: Geological Society of America Bulletin, v. 117, p. 1009–1032, doi:10.1130/B25452.1.

Kokociński, M., Szczuciński, W., Zgrundo, A., and Ibragimow, A., 2009, Diatom assemblages in 26 December 2004 tsunami deposits from coastal zone of Thailand as sediment provenance indicators: Polish Journal of Environmental Studies, v. 18, p. 93–101.

Leonard, L.J., Currie, C.A., Mazzotti, S., and Hyndman, R.D., 2010, Rupture area and displacement of past Cascadia great earthquakes from coastal coseismic subsidence: Geological Society of America Bulletin, v. 122, p. 1951–1968, doi:10.1130/B30108.1.

Manske, D.C., 1968, Distribution of Recent Foraminifera in Relation to Estuarine Hydrography, Yaquina Bay, Oregon [Ph.D. thesis]: Corvallis, Oregon, Oregon State University, 176 p.

Martin, R.A., Nesbit, E.A., and Martin, D.E., 2013, Distribution of foraminifera in Puget Sound, western Washington, U.S.A.: Journal of Foraminiferal Research, v. 43, p. 291–304, doi:10.2113/gsjfr.43.3.291.

Nanayama, N., Furukawa, R., Shigeno, K., Makino, A., Soeda, Y., and Igarashi, Y., 2007, Nine unusually large tsunami deposits from the past 4000 years at Kiritappu marsh along the southern Kuril trench: Sedimentary Geology, v. 200, p. 275–294, doi:10.1016/j.sedgeo.2007.01.008.

National Oceanic and Atmospheric Administration Center for Operational Oceanographic Products and Services (NOAA-COOPS), 2012, South Beach, Yaquina River Coastal Tidal Station Datum: http://tidesandcurrents.noaa.gov/geo.shtml?location=9435380 (accessed April 2012).

Nelson, A.R., and Kashima, K., 1993, Diatom zonation in southern Oregon tidal marshes relative to vascular plants, foraminifera, and sea level: Journal of Coastal Research, v. 9, no. 3, p. 673–697.

Nelson, A.R., Atwater, B.F., Bobrowsky, P.T., Bradley, L.-A., Clague, J.J., Carver, G.A., Darienzo, M.E., Grant, W.C., Krueger, H.W., Sparks, R., Stafford, T.W., Jr., and Stuiver, M., 1995, Radiocarbon evidence for extensive plate-boundary rupture about 300 years ago at the Cascadia subduction zone: Nature, v. 378, p. 371–374, doi:10.1038/378371a0.

Nelson, A.R., Jennings, A.E., and Kashima, K., 1996a, An earthquake history derived from stratigraphic and microfossil evidence of relative sea-level change at Coos Bay, southern coastal Oregon: Geological Society of America Bulletin, v. 108, p. 141–154, doi:10.1130/0016-7606(1996)108<0141:AEHDFS>2.3.CO;2.

Nelson, A.R., Shennan, I., and Long, A.J., 1996b, Identifying coseismic subsidence in tidal-wetland stratigraphic sequences at the Cascadia subduction zone of western North America: Journal of Geophysical Research, v. 101, p. 6115–6135, doi:10.1029/95JB01051.

Nelson, A.R., Ota, Y., Umitsu, M., Kashima, K., and Matsushima, Y., 1998, Seismic or hydrodynamic control of rapid late-Holocene sea-level rises in southern coastal Oregon, USA: The Holocene, v. 8, p. 287–299, doi:10.1191/095968398668600476.

Nelson, A.R., Aspuith, A.C., and Grant, W.C., 2004, Great earthquakes and tsunamis of the past 2000 years at the Salmon River estuary, central Oregon coast, USA: Bulletin of the Seismological Society of America, v. 94, p. 1276–1292, doi:10.1785/012003210.

Nelson, A.R., Kelsey, H.M., and Witter, R.C., 2006, Great earthquakes of variable magnitude at the Cascadia subduction zone: Quaternary Research, v. 65, p. 354–365, doi:10.1016/j.yqres.2006.02.009.

Nelson, A.R., Sawai, Y., Jennings, A.E., Bradley, L., Gerson, L., Sherrod, B.L., Sabean, J., and Horton, B.P., 2008, Great-earthquake paleogeodesy and tsunamis of the past 2,000 years at Alsea Bay, central Oregon coast, USA: Quaternary Science Reviews, v. 27, p. 747–768, doi:10.1016/j.quascirev.2008.01.001.

Parker, R.N., Densmore, A.L., Rosser, N.J., de Michele, M., Yong Li, Y., Huang, R., Whadcoat, S., and Petley, D.N., 2011, Mass wasting triggered by the 2008 Wenchuan earthquake is greater than orogenic growth: Nature Geoscience, v. 4, doi:10.1038/NGEO1154.

Peterson, C.D., and Priest, G.R., 1995, Preliminary reconnaissance of Cascadia paleotsunami deposits in Yaquina Bay, Oregon: Oregon Geology, v. 57, p. 33–40.

Peterson, C.D., Scheidegger, K., and Komar, P., 1984, Sediment composition and hydrography in six high-gradient estuaries of the northwestern United States: Journal of Sedimentary Petrology, v. 54, p. 86–97.

Reimer, P.J., Bard, E., Bayliss, A., Beck, J.W., Blackwell, P.G., Bronk Ramsey, C., Buck, C.E., Cheng, H., Edwards, R.L., Friedrich, M., Grootes, P.M., Guilderson, T.P., Haflidason, H., Hajdas, I., Hatt, C., Heaton, T.J., Hogg, A.G., Hughen, K.A., Kaiser, K.F., Kromer, B., Manning, S.W., Niu, M., Reimer, R.W., Richards, D.A., Scott, E.M., Southon, J.R., Turney, C.S.M., and van der Plicht, J., 2013, IntCal13 and MARINE13 radiocarbon age calibration curves 0–50,000 years cal BP: Radiocarbon, v. 55, p. 1869–1887, doi:10.2458/azu_js_rc.55.16947.

Rizynk, R.Z., 1973, Interstitial diatoms from two tidal flats in Yaquina estuary, Oregon, USA: Botanica Marina, v. XVI, p. 113–138.

Satake, K., 2002, Tsunamis, *in* Lee, W.H.K., Kanamori, H., Jennings, P.C., and Kisslinger, C., eds., International Handbook of Earthquake and Engineering Seismology, Part A: London, Academic Press, p. 437–451.

Sawai, Y., Horton, B.P., and Tamotsu, N., 2004, The development of a diatom-based transfer function along the Pacific coast of eastern Hokkaido, northern Japan—An aid in paleoseismic studies of the Kuril subduction zone: Quaternary Science Reviews, v. 23, p. 2467–2483, doi:10.1016/j.quascirev.2004.05.006.

Sawai, Y., Jankaew, K., Martin, M.E., Pendergast, A., Choowong, M., and Charoentitirat, T., 2009, Diatom assemblages in tsunami deposits associated with the 2004 Indian Ocean tsunami at Phra Thong Island, Thailand: Marine Micropaleontology, v. 73, p. 70–79, B01319, doi:10.1016/j.marmicro.2009.07.003.

Shennan, I., Long, A.J., Rutherford, M.M., Green, F.M., Innes, J.B., Lloyd, J.M., Zong, Y., and Walker, K.J., 1996, Tidal marsh stratigraphy, sea-level change and large earthquakes: A 5000 year record in Washington, U.S.A.: Quaternary Science Reviews, v. 15, p. 1023–1059, doi:10.1016/S0277-3791(96)00007-8.

Shennan, I., Long, A.J., Rutherford, M.M., Innes, J.B., Green, F.M., Kirby, J.R., and Walker, K.J., 1998, Tidal marsh stratigraphy, sea-level change and large earthquakes: II. Submergence events during the last 3500 years at Netarts Bay, Oregon, USA: Quaternary Science Reviews, v. 17, p. 365–393, doi:10.1016/S0277-3791(97)00055-3.

Stuiver, M., and Reimer, P.J., 1993, Extended ^{14}C database and revised CALIB 6.0 ^{14}C age calibration program: Radiocarbon, v. 35, p. 215–230.

Troels-Smith, J., 1955, Characterization of Unconsolidated Sediments: Danmarks Geologiske Undersøgelse, ser. IV, v. 3, no. 10, 72 p.

Wang, P.-L., Engelhart. S.E., Wang, K., Hawkes, A.D., Horton, B.P., Nelson, A.R., and Witter, R.C., 2013, Heterogeneous rupture in the Great Cascadia earthquake of 1700 inferred from coastal subsidence estimates: Journal of Geophysical Research–Solid Earth, v. 118, no. 5, p. 2460–2473, doi:10.1002/jgrb.50101.

Witter, R.C., 2008, Prehistoric Cascadia Tsunami Inundation and Runup at Cannon Beach, Clatsop County, Oregon: Oregon Department of Geology and Mineral Industries Open-File Report O-08-12, 46 p.

Witter, R.C., Kelsey, H.M., and Hemphill-Haley, E., 2003, Great Cascadia earthquakes and tsunamis of the past 6,700 years, Coquille River estuary, southern coastal Oregon: Geological Society of America Bulletin, v. 115, p. 1289–1306, doi:10.1130/B25189.1.

Witter, R.C., Hemphill-Haley, E., Hart, R., and Gay, L., 2009, Tracking Prehistoric Cascadia Tsunami Deposits at Nestucca Bay, Oregon: U.S. Geological Survey, National Earthquake Hazards Reduction Program Final Technical Report 08HQGR0076, 92 p.

Science Editor: A. Hope Jahren
Associate Editor: An Yin

Manuscript Received 30 January 2014
Revised Manuscript Received 30 May 2014
Manuscript Accepted 1 July 2014

Printed in the USA